

AD-A067 260

AERONAUTICAL RESEARCH LABS MELBOURNE (AUSTRALIA)
AN INTRODUCTION TO THE USE OF ISOPARAMETRIC ELEMENTS WITH EXAMP--ETC(U)
AUG 78 B C HOSKIN, B I GREEN
ARL/STRUC-372

F/G 20/11

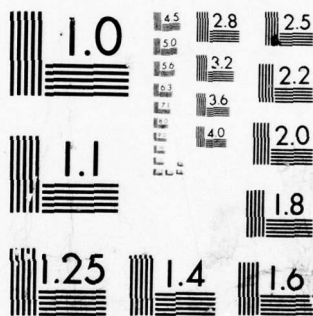
UNCLASSIFIED

NL

| OF /
AD
A067 260
[Small square logo]



END
DATE
FILMED
6 --79
DDC



MICROCOPY RESOLUTION TEST CHART
NATIONAL BUREAU OF STANDARDS-1963-A

UNCLASSIFIED

72 B.S.

ARL-STRUC-REPORT-372

AR-001-292



LEVEL II

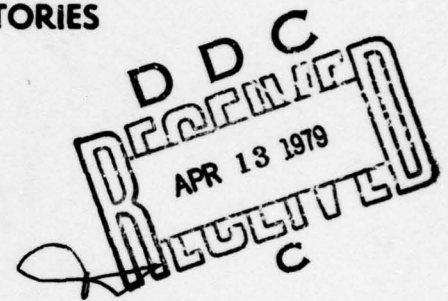
AD A0 67260

DEPARTMENT OF DEFENCE

**DEFENCE SCIENCE AND TECHNOLOGY ORGANISATION
AERONAUTICAL RESEARCH LABORATORIES**

MELBOURNE, VICTORIA

STRUCTURES REPORT 372



**AN INTRODUCTION TO THE USE OF ISOPARAMETRIC
ELEMENTS WITH EXAMPLES FROM THE TORSION
PROBLEM**

by

BRIAN C. HOSKIN and BERYL I. GREEN

DDC FILE COPY

Approved for Public Release.



© COMMONWEALTH OF AUSTRALIA 1978

COPY No 9

79 04 11 056

AUGUST 1978

UNCLASSIFIED

APPROVED
FOR PUBLIC RELEASE

**THE UNITED STATES NATIONAL
TECHNICAL INFORMATION SERVICE
IS AUTHORISED TO
REPRODUCE AND SELL THIS REPORT**

DEPARTMENT OF DEFENCE
DEFENCE SCIENCE AND TECHNOLOGY ORGANISATION
AERONAUTICAL RESEARCH LABORATORIES

14
9
ARL/STRUC-
STRUCTURES REPORT 372

6
AN INTRODUCTION TO THE USE OF ISOPARAMETRIC
ELEMENTS WITH EXAMPLES FROM THE TORSION
PROBLEM.

10
by
BRIAN C. HOSKIN and BERYL I. GREEN

11 Aug 78

12 39p.

SUMMARY

An introductory account is given of the use of isoparametric elements in finite element structural analysis. The basic theory is described and two simple examples are worked out in detail; these both relate to the torsion of bars. Brief mention is also made of other applications of isoparametric elements.

CONTENTS

NOTATION	Page No.
1. INTRODUCTION	1
2. PRINCIPLES OF ISOPARAMETRIC ELEMENTS	1
2.1 General	1
2.2 Interpolation Functions for Square Elements	2
2.3 Mapping Functions	4
3. FORMULATION OF TORSION PROBLEM USING ISOPARAMETRIC ELEMENTS	10
3.1 General	10
3.2 Integral Formulation	10
3.3 Finite Element Formulation	11
3.4 Isoparametric Element Formulation	11
4. ILLUSTRATIVE EXAMPLE USING FOUR-NODE ELEMENTS—TORSION OF BAR WHOSE SECTION IS A RIGHT ANGLE ISOSCELES TRIANGLE	13
4.1 General	13
4.2 Mapping Functions	15
4.3 Element Matrices	17
4.4 Global Equations and Solution	20
5. ILLUSTRATIVE EXAMPLE USING EIGHT-NODE ELEMENTS—TORSION OF BAR WHOSE SECTION IS A QUADRANT OF A CIRCLE	21
5.1 General	21
5.2 Mapping Functions	23
5.3 Element Matrices	24
5.4 Global Equations and Solution	27
6. OTHER APPLICATIONS OF ISOPARAMETRIC ELEMENTS	28
7. CONCLUSIONS	29

DOCUMENT CONTROL DATA

DISTRIBUTION

ACCESSION for	
NTIS	on <input checked="" type="checkbox"/>
BDC	B-4 Section <input type="checkbox"/>
UNANNOUNCED	<input type="checkbox"/>
JUSTIFICATION	
BY	
DISTRIBUTION/ADMINISTRATIVE USES	
DISL	
A	

NOTATION

a_{ij}	Term of element matrix
b_i	Constant term associated with element matrix
u_i, v_i, w_i	See Equations (3.4.5); also Tables 2 and 3
x, y	Co-ordinates in physical plane
x_i, y_i	Co-ordinates of nodal points in physical plane
A, B, C	See Equations (3.4.3)
G	Shear modulus
I	Minimisation integral for cross-section
I_i	Minimisation integral for element
J	Jacobian of mapping function
K	Torsion constant for cross-section
K_i	Torsion constant for element
P_i	Interpolation function for four-node element
Q_i	Interpolation function for eight-node element
ξ, η	Co-ordinates in transformed plane
τ_x, τ_y	Shear stresses in plane of cross-section
$\psi(\xi, \eta)$	Torsion function in transformed plane
$\Psi(x, y)$	Torsion function in physical plane
Ψ_i	Nodal values of torsion function

1. INTRODUCTION

Almost all aircraft structural analysis these days is carried out using computer programs based on the finite element method of analysis. However, at least for the novice user of such programs, there is sometimes an uncertainty about the properties of the various types of elements incorporated in the program libraries. This seems to apply particularly to the so-called "isoparametric elements" even though these were developed around a decade ago^{1,2} and have received some attention in the text book literature.³

Perhaps one of the reasons why uncertainties exist in the case of isoparametric elements is that even simple problems involving them can lead to formidable calculations and in few places can one find illustrative examples worked in detail. It is with these thoughts in mind that the following expository account of isoparametric elements has been prepared. Here, after a review of the basic principles, two illustrative examples are presented at length. In order to keep the calculations of reasonable size both examples relate to the torsion of bars, this being one of the simplest, but still non-trivial, problem types for which isoparametric elements can be usefully employed. (The torsion problem is, for example, simpler than the plane stress problem associated with sheet structures.) Again, to keep the calculations sufficiently concise so that they can be displayed at length, only crude finite element subdivisions are employed and no pretence is made about the precision of the answers for the illustrative examples. Finally, an outline is given of other applications of isoparametric elements, including their use for determining the stress intensity factor in fracture mechanics problems.

2. PRINCIPLES OF ISOPARAMETRIC ELEMENTS

2.1 General

The broad approach in any finite element analysis is to consider the particular region of interest (which, in the illustrative examples to be discussed later, will be the cross-section of a bar in torsion) as subdivided into a finite number of smaller regions, or "elements", these elements being deemed connected at certain points or "nodes". In order to determine how some function of interest (which in the illustrative examples will be the Prandtl torsion function) varies throughout the complete region, a relatively simple form of variation is assumed over each of the elements. The representation thus constructed contains in it, as parameters, the nodal values of the function which is being sought. To this stage then, the problem is basically one of interpolation, and the "interpolation functions" over each element are chosen so that appropriate continuity properties exist at the boundaries of adjacent elements.

The problem now has been reduced to the determination of the nodal values of the sought function. This is achieved by the application of the relevant physical principles which, for elastic problems at least, generally involves the use of a "minimum energy" theorem. Since the strain energy in an elastic body is simply the sum of the strain energy in its constituent parts, the minimisation of the energy can be carried out over the individual elements. Incorporating the results for all elements, a set of simultaneous equations is obtained for the nodal values of the function of interest. After the application of any boundary conditions, these equations can be solved and the problem is then essentially completed.

1. Ergatoudis, I., Irons, B. M., and Zienkiewicz, O. C., Curved Isoparametric Quadrilateral Elements for Finite Element Analysis, *Inter. J. Solids and Structures*, vol. 4, pp. 31-42, 1968.
2. Zienkiewicz, O. C., *et al.*, Isoparametric and Associated Element Families for Two- and Three-Dimensional Analysis, pp. 383-432 of "Finite Element Methods in Stress Analysis", edited by I. Holand and K. Bell, Tapir Forlag, Trondheim, 1970.
3. Gallagher, R. H., *Finite Element Analysis Fundamentals*, Prentice-Hall, Englewood Cliffs, 1975.

The above remarks apply to any finite element problem and, in principle, elements of any shape can be used. However, the practical difficulties associated with the choice of the interpolation functions and with the energy minimisation, which generally involves an integration over the volume of each element, are much reduced when the elements have simple shapes; for example, in two-dimensional problems rectangular or triangular elements are commonly used. The difficulty here is that it may sometimes be necessary to use a large number of such elements in order to give an adequate geometrical representation of the actual region; this is particularly so when the region has curved boundaries. It is under these circumstances that the use of isoparametric elements can be an advantage.

The first, and major, concept with regard to isoparametric elements is that an element of more or less arbitrary shape can be conveniently utilised by "mapping" it on to a simpler shaped region (most commonly, a square); all subsequent calculations are then carried out for this simple region.

The second concept is that the same functional form that is used to effect the mapping can also be used as the interpolation function for the element. It is this use of the same function for the mapping and the interpolation, which gives rise to the name "isoparametric". Although there is no fundamental reason why the same functional form need be used for both purposes, nevertheless it is often the most convenient arrangement in practice; see, for instance, p. 410 of Reference 2.

2.2 Interpolation Functions for Square Elements

The following discussion relates to two-dimensional problems which are to be treated using general "quadrilateral elements". (The sides of the elements may be straight or curved.) For the present purposes, any quadrilateral element in the actual xy plane will be mapped on to the square region defined by

$$\left. \begin{aligned} -1 \leq \xi \leq 1 \\ -1 \leq \eta \leq 1 \end{aligned} \right\} \quad (2.2.1)$$

in the transformed $\xi\eta$ plane; see Figure 1. However, before discussing details of the mapping it will be useful to consider interpolation functions for the transformed region.

2.2.1 Interpolation Functions for Four-Node Square

Suppose the square region in the transformed plane has nodes at each of its corners, identified by the Roman numerals I to IV in Figure 2. Let $\psi(\xi, \eta)$ be some function which is to be expressed throughout this region in terms of its values Ψ_i ($i = \text{I to IV}$) at the nodes. It can be readily verified that this is achieved by the expression

$$\psi(\xi, \eta) = \sum_{i=1}^{\text{IV}} P_i(\xi, \eta) \Psi_i \quad (2.2.2)$$

where

$$\left. \begin{aligned} P_{\text{I}}(\xi, \eta) &= (1 + \xi)(1 + \eta)/4 \\ P_{\text{II}}(\xi, \eta) &= (1 - \xi)(1 + \eta)/4 \\ P_{\text{III}}(\xi, \eta) &= (1 - \xi)(1 - \eta)/4 \\ P_{\text{IV}}(\xi, \eta) &= (1 + \xi)(1 - \eta)/4 \end{aligned} \right\} \quad (2.2.3)$$

At node i , $P_i = 1$ whilst all the other P s are zero. For example, at node I, $\xi = \eta = 1$ and so $P_{\text{I}} = 1$ whilst $P_{\text{II}} = P_{\text{III}} = P_{\text{IV}} = 0$; hence Equation (2.2.2) returns the result $\psi = \Psi_{\text{I}}$ as required. Actually, Equation (2.2.2) is simply the standard formula for linear interpolation over a square region⁴; it implies a linear variation of the function ψ along any straight line parallel to a side of the square.

4. McCormick, J. M., and Salvadori, M. G., Numerical Methods in Fortran, p. 119, Prentice-Hall, Englewood Cliffs, 1964.

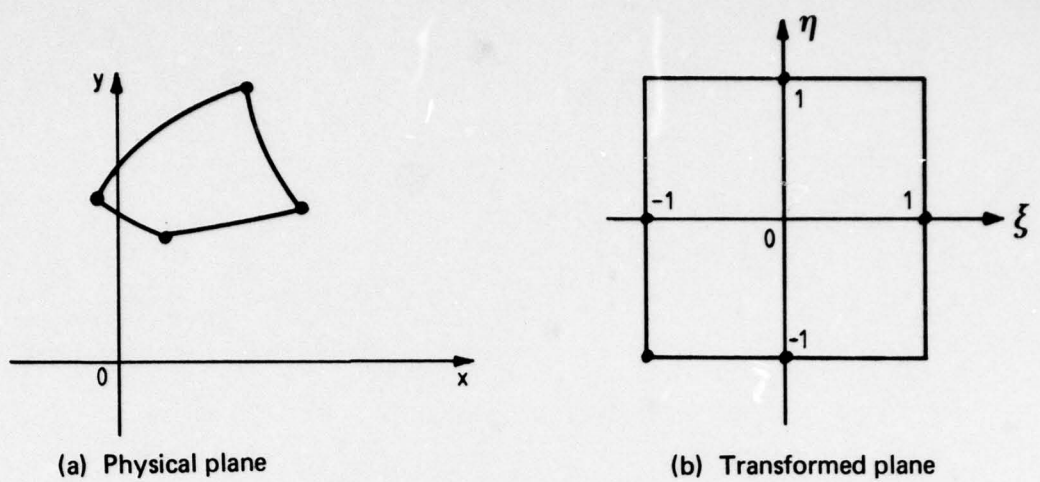


FIG. 1 MAPPING OF GENERAL QUADRILATERAL ELEMENT ON TO SQUARE

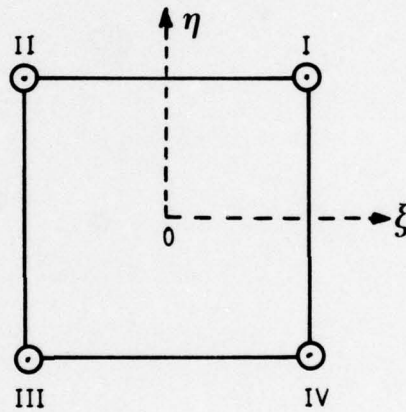


FIG. 2 FOUR NODE SQUARE

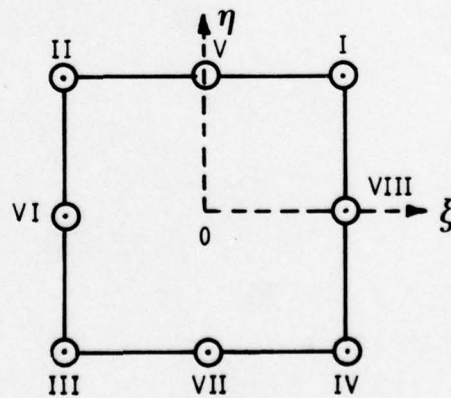


FIG. 3 EIGHT NODE SQUARE

At a later stage, the partial derivatives of ψ with respect to ξ and η will be required:

$$\left. \begin{aligned} \psi_{\xi} &= \{(1 + \eta)(\Psi_I - \Psi_{II}) - (1 - \eta)(\Psi_{III} - \Psi_{IV})\}/4 \\ \psi_{\eta} &= \{(1 + \xi)(\Psi_I - \Psi_{IV}) + (1 - \xi)(\Psi_{II} - \Psi_{III})\}/4 \end{aligned} \right\} \quad (2.2.4)$$

(Note that here and throughout, partial derivatives with respect to ξ and η will be written using the subscript notation.)

2.2.2 Interpolation Functions for Eight-Node Square

Now consider the case where the square in the transformed plane has nodes at the mid-points of each of its sides, as well as at its corners; the midpoint nodes are numbered V to VIII as shown in Figure 3. In this case, the value of ψ at any interior point can be expressed in terms of its nodal values Ψ_i ($i = I$ to VIII) by the relation

$$\psi(\xi, \eta) = \sum_{i=I}^{VIII} Q_i(\xi, \eta) \Psi_i \quad (2.2.5)$$

where

$$\left. \begin{aligned} Q_I(\xi, \eta) &= (1 + \xi)(1 + \eta)(-1 + \xi + \eta)/4 \\ Q_{II}(\xi, \eta) &= (1 - \xi)(1 + \eta)(-1 - \xi + \eta)/4 \\ Q_{III}(\xi, \eta) &= (1 - \xi)(1 - \eta)(-1 - \xi - \eta)/4 \\ Q_{IV}(\xi, \eta) &= (1 + \xi)(1 - \eta)(-1 + \xi - \eta)/4 \\ Q_V(\xi, \eta) &= (1 + \eta)(1 - \xi^2)/2 \\ Q_{VI}(\xi, \eta) &= (1 - \xi)(1 - \eta^2)/2 \\ Q_{VII}(\xi, \eta) &= (1 - \eta)(1 - \xi^2)/2 \\ Q_{VIII}(\xi, \eta) &= (1 + \xi)(1 - \eta^2)/2 \end{aligned} \right\} \quad (2.2.6)$$

Again, it is readily established that, at node i , $Q_i = 1$ whilst all the other Q s are zero, e.g. at node VI, $\xi = -1$ and $\eta = 0$ so $Q_{VI} = 1$, with all other Q s zero. Equation (2.2.5) implies a quadratic variation of ψ along any straight line parallel to a side of the square. However, it should be pointed out that Equation (2.2.5) is not the standard quadratic interpolation formula for a square region, since this last also requires incorporation of a nodal value at the centre of a square (Reference 4).

Analogously to Equation (2.2.4), the partial derivatives of Equation (2.2.5) are

$$\left. \begin{aligned} \psi_{\xi} &= [(1 + \eta)(2\xi + \eta)\Psi_I + (2\xi - \eta)\Psi_{II}] + (1 - \eta)[(2\xi + \eta)\Psi_{III} + (2\xi - \eta)\Psi_{IV}] \\ &\quad - 4\xi[(1 + \eta)\Psi_V + (1 - \eta)\Psi_{VII}] - 2(1 - \eta^2)(\Psi_{VI} - \Psi_{VIII})/4 \\ \psi_{\eta} &= [(1 + \xi)(\xi + 2\eta)\Psi_I + (-\xi + 2\eta)\Psi_{IV}] + (1 - \xi)[(-\xi + 2\eta)\Psi_{II} + (\xi + 2\eta)\Psi_{III}] \\ &\quad + 2(1 - \xi^2)(\Psi_V - \Psi_{VII}) - 4\eta[(1 - \xi)\Psi_{VI} + (1 + \xi)\Psi_{VIII}]/4 \end{aligned} \right\} \quad (2.2.7)$$

2.3 Mapping Functions

Any pair of functional relations of the form

$$\left. \begin{aligned} x &= x(\xi, \eta) \\ y &= y(\xi, \eta) \end{aligned} \right\} \quad (2.3.1)$$

can be interpreted as a mapping of some region in the xy plane on to some other region in the $\xi\eta$ plane. The properties of such mappings are discussed at length in many mathematical texts, e.g. that by Courant.⁵ Before going on to consider specific mapping functions, some of the general results that will be required throughout will be set down.

5. Courant, R., *Differential and Integral Calculus*, vol. II, pp. 133 et seq., Blackie, London, 1936.

If $\Psi(x, y)$ is a function defined over some region R of the xy plane, then on substituting for x and y from Equation (2.3.1), there is obtained a function $\psi(\xi, \eta)$ defined over some other region r of the $\xi\eta$ plane. The following formulae relate the values of integrals and derivatives in the actual plane to those in the transformed plane. For integrals,

$$\iint_R \Psi(x, y) dx dy = \iint_r \psi(\xi, \eta) J(\xi, \eta) d\xi d\eta \quad (2.3.2)$$

where $J(\xi, \eta)$ is the Jacobian of the mapping and is given by

$$J = x_\xi y_\eta - x_\eta y_\xi \quad (2.3.3)$$

For derivatives,

$$\begin{aligned} \Psi_x &= \psi_\xi \xi_x + \psi_\eta \eta_x \\ \Psi_y &= \psi_\xi \xi_y + \psi_\eta \eta_y \end{aligned} \quad (2.3.4)$$

In their present form, the evaluation of the right hand sides of Equations (2.3.4) requires a knowledge of the inverse mapping, i.e. requires the relations

$$\begin{aligned} \xi &= \xi(x, y) \\ \eta &= \eta(x, y) \end{aligned} \quad (2.3.5)$$

However, the need for inverting Equations (2.3.1) to obtain Equations (2.3.5)—which is often not convenient in practice—can be obviated by the use of the relations

$$\begin{aligned} \xi_x &= y_\eta/J & \xi_y &= -x_\eta/J \\ \eta_x &= -y_\xi/J & \eta_y &= x_\xi/J \end{aligned} \quad (2.3.6)$$

where J is, as before, the Jacobian. Hence, substituting from (2.3.6) into (2.3.4) gives

$$\begin{aligned} \Psi_x &= (\psi_\xi y_\eta - \psi_\eta y_\xi)/J \\ \Psi_y &= (-\psi_\xi x_\eta + \psi_\eta x_\xi)/J \end{aligned} \quad (2.3.7)$$

The evaluation of the right hand sides of Equations (2.3.7) only requires a knowledge of the original mapping (2.3.1).

Now attention will be turned to specific mapping functions that are utilised in the case of isoparametric quadrilateral elements.

2.3.1 Mapping of Straight-Sided Quadrilateral on to Square

Consider an arbitrary straight-sided quadrilateral in the xy plane and let x_i, y_i ($i = I$ to IV) denote the co-ordinates of the corners (Fig. 4). Define a mapping by

$$\left. \begin{aligned} x &= \sum_{i=I}^{IV} P_i(\xi, \eta) x_i \\ y &= \sum_{i=I}^{IV} P_i(\xi, \eta) y_i \end{aligned} \right\} \quad (2.3.8)$$

where the P_i are given by Equations (2.2.3). This mapping transforms exactly the quadrilateral into the square region of Figure 2 in the transformed plane. This can be seen as follows. Each corner of the quadrilateral certainly maps into the corresponding corner of the square since $P_i = 1$ at the corner "i" of the square and all the other P s are zero, so Equations (2.3.8) simply return the result $x = x_i, y = y_i$. Further, a side of the quadrilateral maps exactly into a side of the square. For example, the line joining corners I and II of the square corresponds to $\eta = 1$ in the transformed plane. On substituting this value into Equations (2.3.8), these last reduce to

$$\begin{aligned} x &= \{(1 + \xi)x_I + (1 - \xi)x_{II}\}/2 \\ y &= \{(1 + \xi)y_I + (1 - \xi)y_{II}\}/2 \end{aligned} \quad (2.3.9)$$

On eliminating ξ between these equations the result is

$$y(x_{II} - x_I) = x(y_{II} - y_I) + x_{II}y_I - x_Iy_{II} \quad (2.3.10)$$

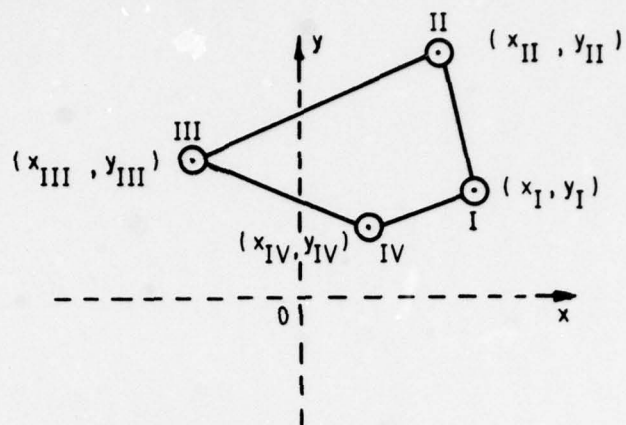


FIG. 4 NODAL COORDINATES FOR STRAIGHT-SIDED QUADRILATERAL

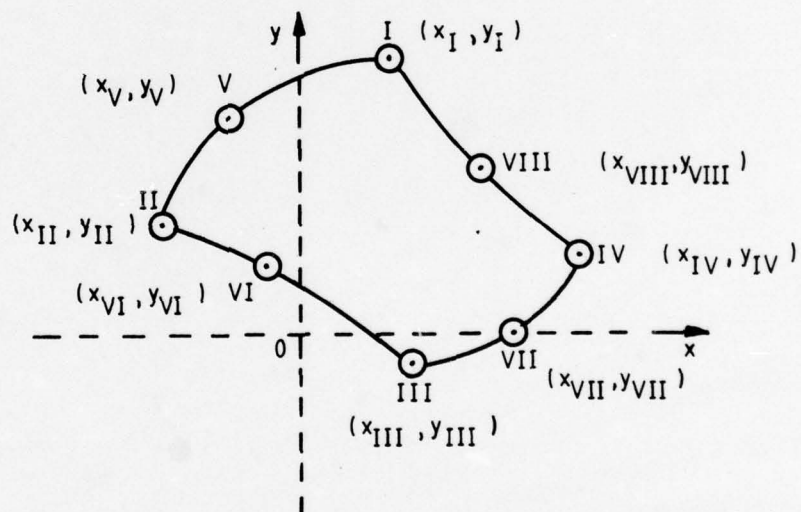


FIG. 5 NODAL COORDINATES FOR CURVILINEAR QUADRILATERAL

This is the equation of the straight line joining the corners I and II of the quadrilateral. Similar results hold for all sides and, hence, Equations (2.3.8) map the sides of the quadrilateral exactly into the sides of the square.

The various derivatives needed for evaluating the Jacobian (2.3.3) and which are also needed in Equations (2.3.7) can be readily obtained from Equation (2.3.8):

$$\left. \begin{aligned} x_{\xi} &= \{(1 + \eta)(x_I - x_{II}) - (1 - \eta)(x_{III} - x_{IV})\}/4 \\ x_{\eta} &= \{(1 + \xi)(x_I - x_{IV}) + (1 - \xi)(x_{II} - x_{III})\}/4 \\ y_{\xi} &= \{(1 + \eta)(y_I - y_{II}) - (1 - \eta)(y_{III} - y_{IV})\}/4 \\ y_{\eta} &= \{(1 + \xi)(y_I - y_{IV}) + (1 - \xi)(y_{II} - y_{III})\}/4 \end{aligned} \right\} \quad (2.3.11)$$

2.3.2 Mapping of Curvilinear Quadrilateral on to Square

Now consider a curvilinear quadrilateral in the xy plane and let x_i, y_i ($i = I$ to IV) denote the co-ordinates of the corners and x_i, y_i ($i = V$ to $VIII$) denote the co-ordinates of intermediate points on the sides of the quadrilateral, ordered as shown in Figure 5. No stipulation is made about particular locations for the intermediate nodes V to $VIII$. Define a mapping by

$$\left. \begin{aligned} x &= \sum_{i=I}^{VIII} Q_i(\xi, \eta) x_i \\ y &= \sum_{i=I}^{VIII} Q_i(\xi, \eta) y_i \end{aligned} \right\} \quad (2.3.12)$$

where the Q s are given by Equations (2.2.6). This mapping transforms approximately the curvilinear quadrilateral in the xy plane into the square of Figure 3 in the $\xi\eta$ plane. By virtue of the properties of the Q s, Equations (2.3.12) will map the eight "nodal" points in the xy plane exactly into the corresponding eight nodal points in the $\xi\eta$ plane. However, in distinction to the situation for a straight-sided quadrilateral, for non-nodal points on the boundary of the square in the $\xi\eta$ plane, the values of x and y as computed from Equations (2.3.12) will not in general lie on the boundary of the curvilinear quadrilateral, i.e. the mapping is not an exact one. (Of course, this could not be expected since the quadrilateral has only been specified to the extent of its eight nodes. Whilst these nodes have uniquely specified the mapping function (2.3.12), they certainly have not uniquely specified the quadrilateral.)

The general nature of the quadrilateral that is being mapped by (2.3.12) can be established by examining what happens as one traverses a side of the square in the $\xi\eta$ plane. For example, referring to Figure 3 it can be seen that the side I-V-II corresponds to $\eta = 1$ and, on substituting this into (2.3.12) the result is

$$\begin{aligned} x &= \xi(1 + \xi)x_I/2 - \xi(1 - \xi)x_{II}/2 + (1 - \xi^2)x_V \\ y &= \xi(1 + \xi)y_I/2 - \xi(1 - \xi)y_{II}/2 + (1 - \xi^2)y_V \end{aligned} \quad (2.3.13)$$

When ξ is eliminated from these two equations, a result of the form

$$c_1x^2 + c_2xy + c_3y^2 + c_4x + c_5y + d = 0 \quad (2.3.14)$$

is obtained, where the coefficients c_j are rather cumbersome functions of the co-ordinates x_i, y_i ($i = I, II, V$). Equation (2.3.14), which represents a second degree curve, defines the boundary curve in the xy plane which is actually being mapped. So far, node V has not been specified in the xy plane beyond the requirement that it lie somewhere along the side I-II. If the choice

$$x_V = (x_I + x_{II})/2 \quad (2.3.15)$$

be made, then the first of Equations (2.3.13) simplifies to

$$x = \{\xi(x_I - x_{II}) + (x_I + x_{II})\}/2 \quad (2.3.16)$$

On eliminating ξ between (2.3.16) and the second of (2.3.13) the result is of the form

$$y = d_1x^2 + d_2x + d_3 \quad (2.3.17)$$

where the coefficients d_j are functions of the x_i and y_i . Here, then, the boundary curve in the xy plane is simply the (unique) parabola through the three nodal points. In this case the accuracy of the mapping is governed by the closeness with which the actual boundary curve can be approximated by a parabola.

However, it is not necessary to make the choice (2.3.15) and, in any given case, the mapping actually being achieved by Equations (2.3.12) can be established by a direct evaluation. As an example, consider the quadrant of a circle of unit radius shown in Figure 6. Later on, the torsion problem for a bar of this cross-section will be worked out in detail using the (coarse) finite element subdivision shown. For the moment attention is restricted to element "b". The nodal numbering along with the nodal co-ordinates for this element are shown in Figure 7. The co-ordinates of the corner nodes are, of course, determined by the finite element subdivision. The intermediate nodes have been selected so as to occur half way along the sides. (In particular, since the arc IV-I subtends an angle of $\pi/4$ at the origin, the arc IV-VIII subtends an angle of $\pi/8$; the relation analogous to (2.3.15) does *not* apply here.) On substituting the values of x_i and y_i as given on Figure 7 into Equations (2.3.12) the mapping function for element "b" is defined. In order to assess the accuracy of the mapping, values of x and y will be calculated from (2.3.12) for various values of ξ and η corresponding to points on the boundary of the square of Figure 3. Attention can be restricted to the curved side IV-VIII-I because the mapping is exact for any straight side, as can easily be proven. The side IV-VIII-I corresponds to

$$\xi = 1, -1 \leq \eta \leq 1 \quad (2.3.18)$$

in the transformed plane. On substituting $\xi = 1$ into (2.3.12) and inserting there the values of x_i and y_i as obtained from Figure 7, the mapping function reduces to

$$x = 0.7071\eta(1 + \eta)/2 - 1.0000\eta(1 - \eta)/2 + 0.9239(1 - \eta^2) \quad (2.3.19)$$

$$y = 0.7071\eta(1 + \eta)/2 + 0 + 0.3827(1 - \eta^2)$$

The result of evaluating (2.3.19) for various values of η is shown in Table 1 below. As a measure of the error in the mapping, the difference, ϵ , between the radius vector from the origin to the mapped point and the radius of the circular boundary (unity) has also been tabulated. Here,

$$\epsilon = (x^2 + y^2)^{1/2} - 1 \quad (2.3.20)$$

It can be seen that the error is everywhere small despite the relatively large length of arc involved. (The error, of course, is zero at the nodal points.)

TABLE 1
Evaluation of Mapping Function for Circular Arc

η	x	y	ϵ
-1.00	1.0000	0.0000	0.0000
-0.75	0.9942	0.1011	-0.0007
-0.50	0.9795	0.1986	-0.0005
-0.25	0.9561	0.2925	-0.0002
0.00	0.9239	0.3827	0.0000
0.25	0.8829	0.4693	-0.0002
0.50	0.8331	0.5522	-0.0005
0.75	0.7745	0.6315	-0.0007
1.00	0.7071	0.7071	0.0000

Finally, the various derivatives needed for use in Equations (2.3.3) and (2.3.7) will be set down:

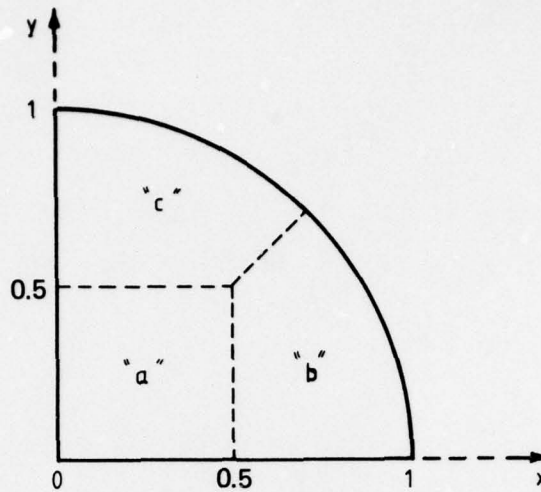


FIG. 6 FINITE ELEMENT SUBDIVISION OF QUADRANT OF CIRCLE OF UNIT RADIUS

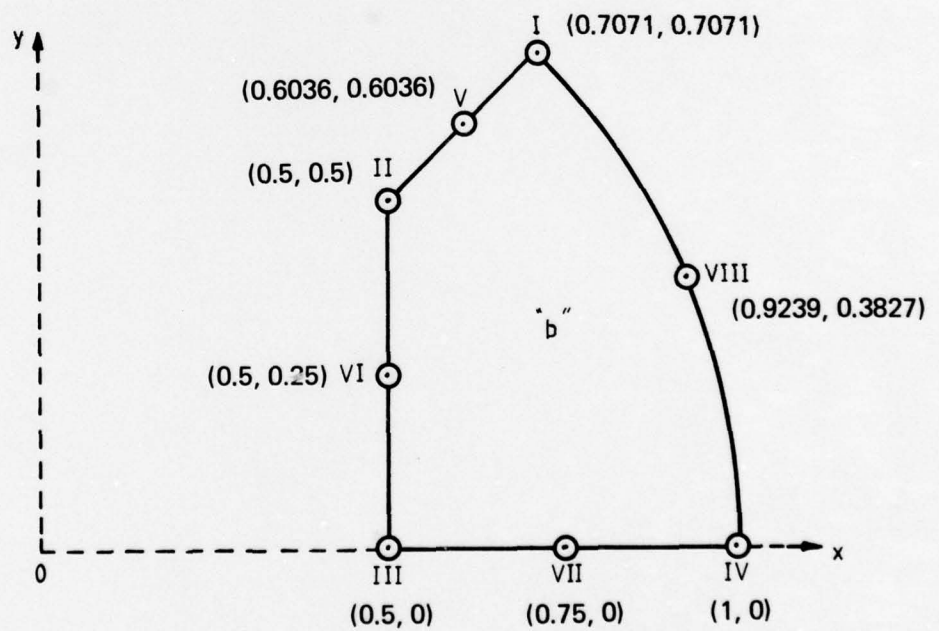


FIG. 7 NODAL COORDINATES FOR ELEMENT 'b'

$$x_\xi = [(1 + \eta)(2\xi + \eta)x_I + (2\xi - \eta)x_{II} + (1 - \eta)(2\xi + \eta)x_{III} + (2\xi - \eta)x_{IV} - 4\xi\{(1 + \eta)x_V + (1 - \eta)x_{VII}\} - 2(1 - \eta^2)(x_{VI} - x_{VIII})]/4 \quad (2.3.21)$$

$$x_\eta = [(1 + \xi)(\xi + 2\eta)x_I + (-\xi + 2\eta)x_{IV} + (1 - \xi)(-\xi + 2\eta)x_{II} + (\xi + 2\eta)x_{III} + 2(1 - \xi^2)(x_V - x_{VII}) - 4\eta\{(1 - \xi)x_{VI} + (1 + \xi)x_{VIII}\}]/4$$

The formulae for y_ξ and y_η are obtained simply by replacing x_i by y_i ($i = I$ to $VIII$) in the above.

3. FORMULATION OF TORSION PROBLEM USING ISOPARAMETRIC ELEMENTS

3.1 General

In the next two Sections the use of isoparametric elements will be demonstrated by examples involving the torsion of bars and it is convenient to set down here the basic equations governing the torsion problem. Consider, therefore, a bar of (constant) cross-section, R , and let c denote the boundary curve of the cross-section. It is shown in standard texts on elasticity, e.g. that by Sokolnikoff,⁶ that the solution of the torsion problem can be reduced to finding a function $\Psi(x, y)$ such that

$$\Psi_{xx} + \Psi_{yy} = -2 \quad \text{over } R \quad (3.1.1)$$

$$\Psi = 0 \quad \text{on } c \quad (3.1.2)$$

where x and y are the co-ordinates in the plane of the cross-section and the suffixes again denote partial differentiation. Once Ψ is determined the torsion constant, K , is given by

$$K = 2 \iint_R \Psi(x, y) dx dy \quad (3.1.3)$$

and the shear stresses τ_x and τ_y by

$$\tau_x/T = \Psi_y/K, \quad \tau_y/T = -\Psi_x/K \quad (3.1.4)$$

where T denotes the applied torque. The angle of twist per unit length, θ , is related to the torque according to

$$T = GK\theta \quad (3.1.5)$$

where G is the shear modulus.

3.2 Integral Formulation

For finite element work, the differential equation formulation embodied in Equation (3.1.1) is not suitable. Instead, use is made of the fact that the function Ψ which satisfies (3.1.1) also makes the integral

$$I(\Psi) = (1/2) \iint_R (\Psi_x^2 + \Psi_y^2 - 4\Psi) dx dy \quad (3.2.1)$$

a minimum. This equivalence can be established either purely mathematically using the Calculus of Variations or, physically, by using the principle of Minimum Complementary Energy (see p. 416 of Ref. 6). The boundary condition (3.1.2), of course, still must be satisfied.

The minimisation required in (3.2.1) is generally carried out as follows. It is assumed that Ψ can be written in the form

$$\Psi(x, y) = \sum_{k=1}^n f_k(x, y) \Psi_k \quad (3.2.2)$$

where the f_k are known functions, and are such that the boundary condition (3.1.2) is satisfied, whilst the Ψ_k are presently unknown parameters. (As will soon transpire, the Ψ_k will be identi-

6. Sokolnikoff, I. S., Mathematical Theory of Elasticity, 2nd edition, p. 116, McGraw-Hill, New York, 1956.

fied with the nodal values of Ψ in a finite element subdivision of the region R .) On substituting from (3.2.2) into (3.2.1) it can be seen that the integral I becomes a function of the Ψ_k , i.e.

$$I(\Psi) = I(\Psi_1, \dots, \Psi_n) \quad (3.2.3)$$

The minimisation of I is achieved by solving the n simultaneous equations

$$\frac{\partial I}{\partial \Psi_k} = 0 \quad k = 1, \dots, n \quad (3.2.4)$$

for the Ψ_k . Once these have been determined the problem is basically solved. (Note that partial differentiation with respect to the Ψ_k will always be denoted by the " ∂ " symbol, rather than a suffix; however, the suffix notation will continue to be used for partial differentiation with respect to x , y , ξ and η .) The above procedure is basically an approximate one, but, in general, the approximation can be rendered adequate by taking a sufficient number of Ψ_k .

3.3 Finite Element Formulation

In the finite element approach to the torsion of a bar, the cross-section R is considered as being subdivided into a number of elements R_l . (A simple example has already been shown in Fig. 6.) Because of the additive nature of integrals it is possible to write, in place of Equation (3.2.1)

$$I = \sum_l I_l \quad (3.3.1)$$

where

$$I_l = (1/2) \iint_{R_l} (\Psi_x^2 + \Psi_y^2 - 4\Psi) dx dy \quad (3.3.2)$$

Then Equations (3.2.4) become

$$\sum_l \frac{\partial I_l}{\partial \Psi_k} = 0 \quad k = 1, \dots, n \quad (3.3.3)$$

Hence, attention is concentrated initially on evaluating the derivatives $\partial I_l / \partial \Psi_k$ for each element; then the final set of equations is obtained by carrying out the summation (3.3.3). From Equation (3.3.2)

$$\frac{\partial I_l}{\partial \Psi_k} = \iint_{R_l} \left(\Psi_x \frac{\partial \Psi_x}{\partial \Psi_k} + \Psi_y \frac{\partial \Psi_y}{\partial \Psi_k} - 2 \frac{\partial \Psi}{\partial \Psi_k} \right) dx dy \quad (3.3.4)$$

In a direct application of the finite element method, some form of variation of Ψ over each element is now assumed, and the integral (3.3.4) is evaluated. However, as already mentioned, there are practical difficulties for any but the simplest shaped elements, firstly, in choosing an appropriate form for Ψ and, secondly, in actually evaluating the integral.

Before passing on it might be noted that the torsion constant K can be written in the form

$$K = \sum_l K_l \quad (3.3.5)$$

where

$$K_l = 2 \iint_{R_l} \Psi(x, y) dx dy \quad (3.3.6)$$

3.4 Isoparametric Element Formulation

Suppose that the subdivision of the cross-section R is made using either the four-node elements of Figure 4 or the eight-node elements of Figure 5. Then, in order to obviate the difficulties just mentioned, each element R_l in the xy plane is, in turn, mapped on to the square region in the $\xi\eta$ plane either by Equation (2.3.8) or by Equation (2.3.12) as appropriate. In this case the function $\Psi(x, y)$ will transform to a function $\psi(\xi, \eta)$ and, using the relations (2.3.2) and (2.3.7), Equation (3.3.4) becomes

$$\begin{aligned} \frac{\partial I_i}{\partial \Psi_i} = \int_{-1}^1 \int_{-1}^1 & \left[\left\{ \left(\psi_\xi y_\eta - \psi_\eta y_\xi \right) \left(\frac{\partial \Psi_\xi}{\partial \Psi_i} y_\eta - \frac{\partial \psi_\eta}{\partial \Psi_i} y_\xi \right) \right. \right. \\ & + \left. \left(-\psi_\xi x_\eta + \psi_\eta x_\xi \right) \left(\frac{-\partial \Psi_\xi}{\partial \Psi_i} x_\eta + \frac{\partial \psi_\eta}{\partial \Psi_i} x_\xi \right) \right\} / J \\ & - 2J \frac{\partial \psi}{\partial \Psi_i} \Big] d\xi d\eta \end{aligned} \quad (3.4.1)$$

Note that, since attention is at present being confined to a single element (the "Ith"), a local nodal numbering system can be used temporarily. Hence, Ψ_i has been written in (3.4.1) in place of Ψ_k in (3.3.4) where i takes the values I to IV for a four-node element and I to VIII for an eight-node element. (Of course, at a later stage the local numbering must be replaced by a global numbering.)

Equation (3.4.1) can be written in the form

$$\frac{\partial I_i}{\partial \Psi_i} = \int_{-1}^1 \int_{-1}^1 \left[\left\{ \left(A \frac{\partial \psi_\xi}{\partial \Psi_i} - B \frac{\partial \psi_\eta}{\partial \Psi_i} \right) \psi_\xi + \left(C \frac{\partial \psi_\eta}{\partial \Psi_i} - B \frac{\partial \psi_\xi}{\partial \Psi_i} \right) \psi_\eta \right\} / J - 2J \frac{\partial \psi}{\partial \Psi_i} \right] d\xi d\eta \quad (3.4.2)$$

where

$$\begin{aligned} A &= x_\eta^2 + y_\eta^2 \\ B &= x_\xi x_\eta + y_\xi y_\eta \\ C &= x_\xi^2 + y_\xi^2 \end{aligned} \quad (3.4.3)$$

Whilst Equation (3.4.2) may appear more formidable than Equation (3.3.4) its evaluation is straightforward, albeit tedious. Depending on the type of element being used, ψ is taken either in the form (2.2.2) or (2.2.5), with ψ_ξ and ψ_η correspondingly being given by either (2.2.4) or (2.2.7). In both cases one can write

$$\begin{aligned} \psi_\xi &= \sum_j u_j \Psi_j \\ \psi_\eta &= \sum_j v_j \Psi_j \\ \psi &= \sum_j w_j \Psi_j \end{aligned} \quad (3.4.4)$$

where the u s, v s and w s are functions of ξ and η whose explicit forms can be obtained from the equations just cited; these are listed in Tables 2 and 3 below. Clearly,

$$u_i = \partial \psi_\xi / \partial \Psi_i, \quad v_i = \partial \psi_\eta / \partial \Psi_i, \quad w_i = \partial \psi / \partial \Psi_i \quad (3.4.5)$$

In Equations (3.4.4) the summation goes from $j = I$ to IV for a four-node element and from $j = I$ to VIII for an eight-node element. On substituting from (3.4.4) into (3.4.2) it follows that

$$\frac{\partial I_i}{\partial \Psi_i} = \sum_j a_{ij} \Psi_j - b_i \quad (3.4.6)$$

where

$$a_{ij} = \int_{-1}^1 \int_{-1}^1 \{ (A u_i - B v_i) u_j + (C v_i - B u_i) v_j \} / J d\xi d\eta \quad (3.4.7)$$

$$b_i = 2 \int_{-1}^1 \int_{-1}^1 w_i J d\xi d\eta \quad (3.4.8)$$

The integrations (3.4.7) and (3.4.8) are virtually always done numerically using a Gaussian integration formula.⁷

7. Hildebrand, F. B., Introduction to Numerical Analysis, McGraw-Hill, New York, 1956.

TABLE 2
Formulae for u_i , v_i , w_i for Four-Node Element

i	u_i	v_i	w_i
I	$(1 + \eta)/4$	$(1 + \xi)/4$	$(1 + \xi)(1 + \eta)/4$
II	$-(1 + \eta)/4$	$(1 - \xi)/4$	$(1 - \xi)(1 + \eta)/4$
III	$-(1 - \eta)/4$	$-(1 - \xi)/4$	$(1 - \xi)(1 - \eta)/4$
IV	$(1 - \eta)/4$	$-(1 + \xi)/4$	$(1 + \xi)(1 - \eta)/4$

TABLE 3
Formulae for u_i , v_i , w_i for Eight-Node Element

i	u_i	v_i	w_i
I	$(1 + \eta)(2\xi + \eta)/4$	$(1 + \xi)(\xi + 2\eta)/4$	$(1 + \xi)(1 + \eta)(-1 + \xi + \eta)/4$
II	$(1 + \eta)(2\xi - \eta)/4$	$(1 - \xi)(-\xi + 2\eta)/4$	$(1 - \xi)(1 + \eta)(-1 - \xi + \eta)/4$
III	$(1 - \eta)(2\xi + \eta)/4$	$(1 - \xi)(\xi + 2\eta)/4$	$(1 - \xi)(1 - \eta)(-1 - \xi - \eta)/4$
IV	$(1 - \eta)(2\xi - \eta)/4$	$(1 + \xi)(-\xi + 2\eta)/4$	$(1 + \xi)(1 - \eta)(-1 + \xi - \eta)/4$
V	$-\xi(1 + \eta)$	$(1 - \xi^2)/2$	$(1 + \eta)(1 - \xi^2)/2$
VI	$-(1 - \eta^2)/2$	$-\eta(1 - \xi)$	$(1 - \xi)(1 - \eta^2)/2$
VII	$-\xi(1 - \eta)$	$-(1 - \xi^2)/2$	$(1 - \eta)(1 - \xi^2)/2$
VIII	$(1 - \eta^2)/2$	$-\eta(1 + \xi)$	$(1 + \xi)(1 - \eta^2)/2$

When the quantities a_{ij} and b_i have been determined for each element, the global equations (3.3.3) can be set up. The boundary condition (3.1.2) is then applied by setting $\Psi_k = 0$ for each boundary node. After solving the resulting set of equations for the remaining Ψ_k the problem is essentially complete. The torsion constant K can be computed from Equation (3.3.5) where now, in place of Equation (3.3.6)

$$K_I = 2 \int_{-1}^1 \int_{-1}^1 \psi(\xi, \eta) J(\xi, \eta) d\xi d\eta \quad (3.4.9)$$

On substituting from the third of Equations (3.4.4) into Equation (3.4.9), and using Equation (3.4.8), it follows that

$$K_I = \sum b_i \Psi_i \quad (3.4.10)$$

the summation going either from I to IV or I to VIII.

The stresses can be obtained by substituting from Equations (2.3.7) into Equations (3.1.4) to get

$$\begin{aligned} \tau_x/T &= (-\psi_\xi x_\eta + \psi_\eta x_\xi)/(JK) \\ \tau_y/T &= -(\psi_\xi y_\eta - \psi_\eta y_\xi)/(JK) \end{aligned} \quad (3.4.11)$$

4. ILLUSTRATIVE EXAMPLE USING FOUR-NODE ELEMENTS—TORSION OF BAR WHOSE SECTION IS A RIGHT ANGLE ISOSCELES TRIANGLE

4.1 General

As an example of the use of four-node isoparametric elements, the torsion of a bar having a cross-section in the form of a right-angle isosceles triangle will be considered. The vertices of the triangle are located at the points (1, 0), (0, 1), (-1, 0) as shown in Figure 8. The (crude) finite element subdivision adopted is shown in Figure 9, the elements being identified as "a",

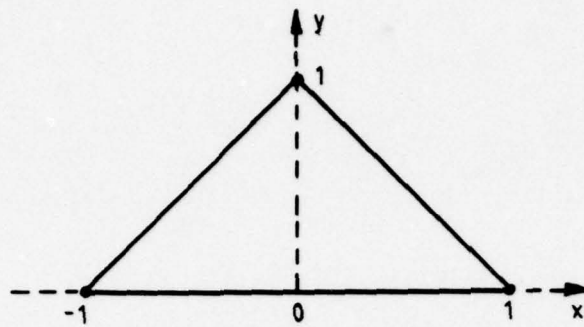
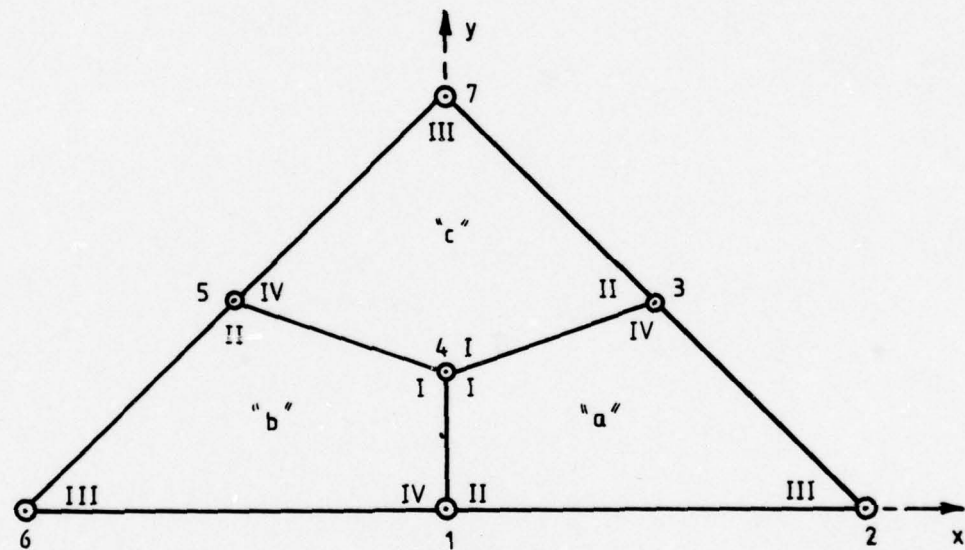


FIG. 8 CROSS SECTION OF BAR FOR ILLUSTRATIVE EXAMPLE OF SECTION 4



Global nodes numbered in ordinary numerals
Local (element) nodes numbered in Roman numerals

FIG. 9 FINITE ELEMENT SUBDIVISION, WITH NODAL NUMBERS, FOR ILLUSTRATIVE EXAMPLE OF SECTION 4

"b" and "c". Also shown in Figure 9 are the global node numbers (1 to 7) and the local node numbers for each element (I to IV). These last must run sequentially in a counter-clockwise sense within any one element; however, node I can be assigned arbitrarily. The co-ordinates of the nodes are as shown in Table 4 below.

TABLE 4
Nodal Co-ordinates for Triangle

Element node no.	Element a			Element b			Element c		
	Global node no.	x_i	y_i	Global node no.	x_i	y_i	Global node no.	x_i	y_i
I	4	0	0.3333	4	0	0.3333	4	0	0.3333
II	1	0	0	5	-0.5	0.5	3	0.5	0.5
III	2	1	0	6	-1	0	7	0	1
IV	3	0.5	0.5	1	0	0	5	-0.5	0.5

Table 4 contains all the data needed for the construction of the mapping functions and their derivatives. However, before passing on to these, some reference should be made to the numerical integration scheme which will be used throughout this Section and the next. The determination of the a_{ij} and b_i which are defined by Equations (3.4.7) and (3.4.8) always requires the evaluation of an integral of the form

$$F = \int_{-1}^1 \int_{-1}^1 f(\xi, \eta) d\xi d\eta \quad (4.1.1)$$

Here, the four-point Gaussian formula, namely,

$$F \approx f(-1/\sqrt{3}, -1/\sqrt{3}) + f(1/\sqrt{3}, -1/\sqrt{3}) + f(-1/\sqrt{3}, 1/\sqrt{3}) + f(1/\sqrt{3}, 1/\sqrt{3}) \quad (4.1.2)$$

will always be used. In practice, a higher order formula, e.g. the nine-point formula, should generally be used but (4.1.2) will serve to illustrate the nature of the calculations.

4.2 Mapping Functions

Actually, the mapping functions for the various elements are not required anywhere in the calculations; it is only the derivatives of the mapping functions which appear. However, for completeness they will be included here. Each element will be considered in turn.

Element a

Substituting the values of x_i and y_i ($i = I$ to IV) from Table 4 into Equations (2.3.8) gives

$$x = \{(1 + \xi)(1 + \eta)(0) + (1 - \xi)(1 + \eta)(0) + (1 - \xi)(1 - \eta)(1) + (1 + \xi)(1 - \eta)(0.5)\}/4$$

$$y = \{(1 + \xi)(1 + \eta)(0.3333) + (1 - \xi)(1 + \eta)(0) + (1 - \xi)(1 - \eta)(0) + (1 + \xi)(1 - \eta)(0.5)\}/4$$

These simplify to

$$x = 0.375 - 0.125\xi - 0.375\eta + 0.125\xi\eta \quad (4.2.1)$$

$$y = 0.2083 + 0.2083\xi - 0.0416\eta - 0.0416\xi\eta$$

The derivatives of the mapping function as calculated from Equations (2.3.11) (or from (4.2.1)) are

$$\begin{aligned} x_\xi &= -0.125(1 - \eta) & x_\eta &= -0.125(3 - \xi) \\ y_\xi &= 0.0416(5 - \eta) & y_\eta &= -0.0416(1 + \xi) \end{aligned} \quad (4.2.2)$$

(It might be observed that all calculations were done using more figures than will be displayed here; the displayed numbers here and throughout have been obtained by truncating, rather than rounding, the actual numbers. This gives rise to some apparent discrepancies of a minor nature.)

It is now necessary to evaluate the derivatives (4.2.2) for values of ξ and η corresponding to the points utilised in the Gaussian integration. The results are shown in Table 5.

TABLE 5
Derivatives of Mapping Function for Element a

ξ, η	$-1/\sqrt{3}, -1/\sqrt{3}$	$1/\sqrt{3}, -1/\sqrt{3}$	$-1/\sqrt{3}, 1/\sqrt{3}$	$1/\sqrt{3}, 1/\sqrt{3}$
x_ξ	-0.1971	-0.1971	-0.0528	-0.0528
x_η	-0.4471	-0.3028	-0.4471	-0.3028
y_ξ	0.2323	0.2323	0.1842	0.1842
y_η	-0.0176	-0.0657	-0.0176	-0.0657

The values of Table 5 are, in turn, used to calculate the quantities J , from Equation (2.3.3), and A, B, C from Equations (3.4.3). The results are shown in Table 6.

TABLE 6
Values of J, A, B, C for Element a

ξ, η	$-1/\sqrt{3}, -1/\sqrt{3}$	$1/\sqrt{3}, -1/\sqrt{3}$	$-1/\sqrt{3}, 1/\sqrt{3}$	$1/\sqrt{3}, 1/\sqrt{3}$
J	0.1073	0.0833	0.0833	0.0592
A	0.2002	0.0960	0.2002	0.0960
B	0.0840	0.0445	0.0203	0.0038
C	0.0928	0.0928	0.0367	0.0367

Element b

There is no need to carry out any calculations for element b, because the final result for it can be determined from that for element a by appealing to symmetry.

Element c

Again the mapping function will be displayed. Using the values from Table 4, appropriate to element c, this is found to be

$$x = 0.25(-\xi + \eta) \quad (4.2.3)$$

$$y = 0.0833(7 - 2\xi - 2\eta + \xi\eta)$$

The derivatives of the mapping function as calculated from Equations (2.3.11) (or (4.2.3)) are

$$x_\xi = -0.25 \quad x_\eta = 0.25 \quad (4.2.4)$$

$$y_\xi = 0.0833(-2 + \eta) \quad y_\eta = 0.0833(-2 + \xi)$$

The values of these derivatives at the points used in the Gaussian integration are shown in Table 7 and the subsequently calculated values of the quantities J, A, B and C are shown in Table 8.

TABLE 7
Derivatives of Mapping Function for Element c

ξ, η	$-1/\sqrt{3}, -1/\sqrt{3}$	$1/\sqrt{3}, -1/\sqrt{3}$	$-1/\sqrt{3}, 1/\sqrt{3}$	$1/\sqrt{3}, 1/\sqrt{3}$
x_ξ	-0.2500	-0.2500	-0.2500	-0.2500
x_η	0.2500	0.2500	0.2500	0.2500
y_ξ	-0.2147	-0.2147	-0.1185	-0.1185
y_η	-0.2147	-0.1185	-0.2147	-0.1185

TABLE 8
Values of J, A, B, C for Element c

ξ, η	$-1/\sqrt{3}, -1/\sqrt{3}$	$1/\sqrt{3}, -1/\sqrt{3}$	$-1/\sqrt{3}, 1/\sqrt{3}$	$1/\sqrt{3}, 1/\sqrt{3}$
J	0.1073	0.0833	0.0833	0.0592
A	0.1086	0.0765	0.1086	0.0765
B	-0.0163	-0.0370	-0.0370	-0.0484
C	0.1086	0.1086	0.0765	0.0765

4.3 Element Matrices

The next stage of the calculation is the determination of the quantities a_{ij} and b_i , as defined by Equations (3.4.7) and (3.4.8) for each element. The a_{ij} , of course, are the components of a symmetric 4×4 matrix for each element. However, it is convenient to first evaluate the quantities u_i , v_i , and w_i (defined in Table 2) at the points used in the Gaussian integration, since these have the same values for all elements. The results are shown in Tables 9, 10 and 11 below.

TABLE 9
Value of u_i at Integration Points

i	ξ, η	$-1/\sqrt{3}, -1/\sqrt{3}$	$1/\sqrt{3}, -1/\sqrt{3}$	$-1/\sqrt{3}, 1/\sqrt{3}$	$1/\sqrt{3}, 1/\sqrt{3}$
I		0.1056	0.1056	0.3943	0.3943
II		-0.1056	-0.1056	-0.3943	-0.3943
III		-0.3943	-0.3943	-0.1056	-0.1056
IV		0.3943	0.3943	0.1056	0.1056

TABLE 10
Values of v_i at Integration Points

i	ξ, η	$-1/\sqrt{3}, -1/\sqrt{3}$	$1/\sqrt{3}, -1/\sqrt{3}$	$-1/\sqrt{3}, 1/\sqrt{3}$	$1/\sqrt{3}, 1/\sqrt{3}$
I		0.1056	0.3943	0.1056	0.3943
II		0.3943	0.1056	0.3943	0.1056
III		-0.3943	-0.1056	-0.3943	-0.1056
IV		-0.1056	-0.3943	-0.1056	-0.3943

TABLE 11
Values of w_i at Integration Points

i	ξ, η	$-1/\sqrt{3}, -1/\sqrt{3}$	$1/\sqrt{3}, -1/\sqrt{3}$	$-1/\sqrt{3}, 1/\sqrt{3}$	$1/\sqrt{3}, 1/\sqrt{3}$
I		0.0446	0.1666	0.1666	0.6220
II		0.1666	0.0446	0.6220	0.1666
III		0.6220	0.1666	0.1666	0.0446
IV		0.1666	0.6220	0.0446	0.1666

For the remainder of the calculations it is necessary to consider each element individually.

Element a

As an intermediate step, the quantities $(Au_i - Bv_i)$ and $(Cv_i - Bu_i)$ are calculated at the integration points using the values given in Tables 6, 9 and 10. The results are shown in Tables 12 and 13 below.

TABLE 12
Values of $(Au_i - Bv_i)$ at Integration Points

i	ξ, η	$-1/\sqrt{3}, -1/\sqrt{3}$	$1/\sqrt{3}, -1/\sqrt{3}$	$-1/\sqrt{3}, 1/\sqrt{3}$	$1/\sqrt{3}, 1/\sqrt{3}$
I		0.0122	-0.0074	0.0768	0.0363
II		-0.0543	-0.0148	-0.0870	-0.0382
III		-0.0458	-0.0331	-0.0131	-0.0097
IV		0.0878	0.0554	0.0233	0.0116

TABLE 13
Values of $(Cv_i - Bu_i)$ at Integration Points

i	ξ, η	$-1/\sqrt{3}, -1/\sqrt{3}$	$1/\sqrt{3}, -1/\sqrt{3}$	$-1/\sqrt{3}, 1/\sqrt{3}$	$1/\sqrt{3}, 1/\sqrt{3}$
I		0.0009	0.0319	-0.0041	0.0129
II		0.0455	0.0145	0.0225	0.0054
III		-0.0034	0.0077	-0.0123	-0.0034
IV		-0.0429	-0.0542	-0.0060	-0.0149

Recalling Equation (4.1.2), the a_{ij} and b_i for element a can now be evaluated using Equations (3.4.7) and (3.4.8) in conjunction with the numerical values given in Tables 6, 9, 10, 11, 12 and 13. Three typical calculations are reproduced below.

$$\begin{aligned} a_{11} &= (0.0122 \times 0.1056 + 0.0009 \times 0.1056)/(0.1073) \\ &\quad + (-0.0074 \times 0.1056 + 0.0319 \times 0.3943)/(0.0833) \\ &\quad + (0.0768 \times 0.3943 - 0.0041 \times 0.1056)/(0.0833) \\ &\quad + (0.0363 \times 0.3943 + 0.0129 \times 0.3943)/(0.0592) \\ &= 0.8407 \end{aligned}$$

$$\begin{aligned} a_{34} &= (-0.0458 \times 0.3943 + 0.0034 \times 0.1056)/(0.1073) \\ &\quad + (-0.0331 \times 0.3943 - 0.0077 \times 0.3943)/(0.0833) \\ &\quad + (-0.0131 \times 0.1056 + 0.0123 \times 0.1056)/(0.0833) \\ &\quad + (-0.0097 \times 0.1056 + 0.0034 \times 0.3943)/(0.0592) \\ &= -0.3537 \end{aligned}$$

$$\begin{aligned} b_2 &= 2(0.1666 \times 0.1073 + 0.0446 \times 0.0833 + 0.6220 \times 0.0833 \\ &\quad + 0.1666 \times 0.0592) = 0.1666 \end{aligned}$$

By proceeding in this way the full set of equations for element a is found to be

$$\begin{bmatrix} \partial I_a / \partial \Psi_I \\ \partial I_a / \partial \Psi_{II} \\ \partial I_a / \partial \Psi_{III} \\ \partial I_a / \partial \Psi_{IV} \end{bmatrix} = \begin{bmatrix} 0.8407 & -0.5605 & -0.2194 & -0.0607 \\ -0.5605 & 1.0404 & 0.1464 & -0.6263 \\ -0.2194 & 0.1464 & 0.4266 & -0.3537 \\ -0.0607 & -0.6263 & -0.3537 & 1.0404 \end{bmatrix} \begin{bmatrix} \Psi_I \\ \Psi_{II} \\ \Psi_{III} \\ \Psi_{IV} \end{bmatrix} - \begin{bmatrix} 0.1388 \\ 0.1666 \\ 0.1944 \\ 0.1666 \end{bmatrix} \quad (4.3.1)$$

Using the correspondence between local nodes and global nodes given in Table 4 these last equations can be written as

$$\begin{bmatrix} \partial I_a / \partial \Psi_4 \\ \partial I_a / \partial \Psi_1 \\ \partial I_a / \partial \Psi_2 \\ \partial I_a / \partial \Psi_3 \end{bmatrix} = \begin{bmatrix} 0.8407 & -0.5605 & -0.2194 & -0.0607 \\ -0.5605 & 1.0404 & 0.1464 & -0.6263 \\ -0.2194 & 0.1464 & 0.4266 & -0.3537 \\ -0.0607 & -0.6263 & -0.3537 & 1.0404 \end{bmatrix} \begin{bmatrix} \Psi_4 \\ \Psi_1 \\ \Psi_2 \\ \Psi_3 \end{bmatrix} - \begin{bmatrix} 0.1388 \\ 0.1666 \\ 0.1944 \\ 0.1666 \end{bmatrix} \quad (4.3.2)$$

Element b

As already remarked the results for element b can be written down by utilising symmetry. Referring to Figure 9 it can be seen that nodes 4, 1, 2 and 3 in element a correspond respectively to nodes 4, 1, 6 and 5 in element b. Hence, on making the necessary changes in Equation (4.3.2), the results for element b become

$$\begin{bmatrix} \partial I_b / \partial \Psi_4 \\ \partial I_b / \partial \Psi_1 \\ \partial I_b / \partial \Psi_6 \\ \partial I_b / \partial \Psi_5 \end{bmatrix} = \begin{bmatrix} 0.8407 & -0.5605 & -0.2194 & -0.0607 \\ -0.5605 & 1.0404 & 0.1464 & -0.6263 \\ -0.2194 & 0.1464 & 0.4266 & -0.3537 \\ -0.0607 & -0.6263 & -0.3537 & 1.0404 \end{bmatrix} \begin{bmatrix} \Psi_4 \\ \Psi_1 \\ \Psi_6 \\ \Psi_5 \end{bmatrix} - \begin{bmatrix} 0.1388 \\ 0.1666 \\ 0.1944 \\ 0.1666 \end{bmatrix} \quad (4.3.3)$$

Element c

The calculations for element c are quite analogous to those for element a. The quantities $(Au_i - Bv_i)$ and $(Cv_i - Bu_i)$ need to be recalculated using the values given in Tables 8, 9 and 10. The a_{ij} and b_i are then calculated as before. Only the final result will be cited here.

$$\begin{bmatrix} \partial I_c / \partial \Psi_4 \\ \partial I_c / \partial \Psi_3 \\ \partial I_c / \partial \Psi_7 \\ \partial I_c / \partial \Psi_5 \end{bmatrix} = \begin{bmatrix} 1.1818 & -0.2878 & -0.6060 & -0.2878 \\ -0.2878 & 0.5252 & -0.0959 & -0.1414 \\ -0.6060 & -0.0959 & 0.7979 & -0.0959 \\ -0.2878 & -0.1414 & -0.0959 & 0.5252 \end{bmatrix} \begin{bmatrix} \Psi_4 \\ \Psi_3 \\ \Psi_7 \\ \Psi_5 \end{bmatrix} - \begin{bmatrix} 0.1388 \\ 0.1666 \\ 0.1944 \\ 0.1666 \end{bmatrix} \quad (4.3.4)$$

4.4 Global Equations and Solution

It is now possible to set up the global Equations (3.3.3) simply by the appropriate addition of Equations (4.3.2), (4.3.3) and (4.3.4). Each global equation is of the form

$$\frac{\partial I}{\partial \Psi_k} = \frac{\partial I_a}{\partial \Psi_k} + \frac{\partial I_b}{\partial \Psi_k} + \frac{\partial I_c}{\partial \Psi_k} = 0 \quad (4.4.1)$$

For example, the equation $\partial I / \partial \Psi_1 = 0$ is obtained by adding the second of Equation (4.3.2) to the second of Equation (4.3.3), there being no contribution from Equation (4.3.4). The full set of equations is shown below:

$$\begin{bmatrix} 2.080 & 0.146 & -0.626 & -1.121 & -0.626 & 0.146 & 0 \\ 0.146 & 0.426 & -0.353 & -0.219 & 0 & 0 & 0 \\ -0.626 & -0.353 & 1.566 & -0.348 & -0.141 & 0 & -0.095 \\ -1.121 & -0.219 & -0.348 & 2.863 & -0.348 & -0.219 & -0.606 \\ -0.626 & 0 & -0.141 & -0.348 & 1.566 & -0.353 & -0.095 \\ 0.146 & 0 & 0 & -0.219 & -0.353 & 0.426 & 0 \\ 0 & 0 & -0.095 & -0.606 & -0.095 & 0 & 0.797 \end{bmatrix} \begin{bmatrix} \Psi_1 \\ \Psi_2 \\ \Psi_3 \\ \Psi_4 \\ \Psi_5 \\ \Psi_6 \\ \Psi_7 \end{bmatrix} = \begin{bmatrix} 0.333 \\ 0.194 \\ 0.333 \\ 0.416 \\ 0.333 \\ 0.194 \\ 0.194 \end{bmatrix} \quad (4.4.2)$$

At this stage the boundary condition (3.1.2) is applied. Because of the extreme simplicity of the present example all nodes, save node 4, are boundary nodes and for each of these $\Psi_k = 0$; also the corresponding equations $\partial I / \partial \Psi_k = 0$ are discarded. Hence (4.4.2) reduce to the single equation

$$2.863\Psi_4 = 0.416 \quad (4.4.3)$$

with the solution $\Psi_4 = 0.145$. (Incidentally, an analytical solution for the torsion function is given in Reference 6 and, from this, the exact value $\Psi_4 = 0.116$ can be found.)

Since, over each element, $\psi(\xi, \eta)$ is given by Equation (2.2.2) and since, from Table 4, global node 4 corresponds to local node I in all three elements (coincidentally), it follows that in each element, on setting $\Psi_I = 0.145$ with all other $\Psi_i = 0$,

$$\psi(\xi, \eta) = 0.145P_I(\xi, \eta) = 0.145(1 + \xi)(1 + \eta)/4 \quad (4.4.4)$$

The torsion constant K_i for each element can be obtained from Equation (3.4.10). For example

$$K_a = b_I\Psi_I + b_{II}\Psi_{II} + b_{III}\Psi_{III} + b_{IV}\Psi_{IV} \quad (4.4.5)$$

which, on extracting the value for b_I from Equation (4.3.1), and bearing in mind that only Ψ_I is non-zero, reduces to

$$K_a = 0.1388 \times 0.145 = 0.0202 \quad (4.4.6)$$

The values of K_b and K_c turn out to be the same, so that the torsion constant for the complete section obtained by carrying out the summation (3.3.5) is

$$K = 0.0606 \quad (4.4.7)$$

(The exact answer as given by Roark⁸ is 0.1044.)

8. Roark, R. J., Formulas for Stress and Strain, 3rd ed., p. 179, McGraw-Hill, New York, 1954.

Finally, the stress, τ_x , at node 1 will be calculated, treating node 1 as belonging to element a. The general formula is given by (3.4.11). Since global node 1 corresponds to local node II in element a, for the present calculations $\xi = -1$, $\eta = 1$. From Equation (4.2.2) the derivatives of the mapping function at this point have the following values:

$$x_\xi = 0 \quad x_\eta = -0.500 \quad (4.4.8)$$

$$y_\xi = 0.166 \quad y_\eta = 0$$

with the Jacobian $J = 0.0833$, from Equation (2.3.3). Also, from Equation (4.4.4)

$$\psi_\xi(-1, 1) = 0.145(1 + \eta)/4 = 0.0727 \quad (4.4.9)$$

$$\psi_\eta(-1, 1) = 0.145(1 + \xi)/4 = 0$$

Using these values in Equation (3.4.11), with K having the value 0.0606 from Equation (4.4.7), gives the result

$$\tau_x/T = 7.19 \quad (4.4.10)$$

(The exact answer as given in Reference 8 is 6.38.)

5. ILLUSTRATIVE EXAMPLE USING EIGHT-NODE ELEMENTS—TORSION OF BAR WHOSE SECTION IS A QUADRANT OF A CIRCLE

5.1 General

As an example of the use of eight-node isoparametric elements, the torsion of a bar whose cross-section comprises a quadrant of a circle of unit radius will be considered (Fig. 10). The finite element subdivision adopted is shown in Figure 11, the elements again being identified as "a", "b" and "c". Also shown in Figure 11 are the global node numbers (1–16) and the local node numbers (I–VIII) for each element. These last must follow the sequence indicated in the counter-clockwise sense, in each element. The co-ordinates of the nodes are as shown in Table 14 below. (As indicated earlier in Section 2.3.2 all the intermediate nodes have been located at the half-way points of the sides.)

TABLE 14
Nodal Co-ordinates for Quadrant

Element node no.	Element a			Element b			Element c		
	Global node no.	x_i	y_i	Global node no.	x_i	y_i	Global node no.	x_i	y_i
I	11	0.5	0.5	13	0.707	0.707	13	0.707	0.707
II	9	0	0.5	11	0.5	0.5	16	0	1.0
III	1	0	0	3	0.5	0	9	0	0.5
IV	3	0.5	0	5	1.0	0	11	0.5	0.5
V	10	0.25	0.5	12	0.603	0.603	15	0.382	0.923
VI	6	0	0.25	7	0.5	0.25	14	0	0.75
VII	2	0.25	0	4	0.75	0	10	0.25	0.5
VIII	7	0.5	0.25	8	0.923	0.382	12	0.603	0.603

The calculations for the present case follow a very similar pattern to those described at length in Section 4 and, again, all integrations will be carried out using the formula (4.1.2). The description here will be somewhat more concise.

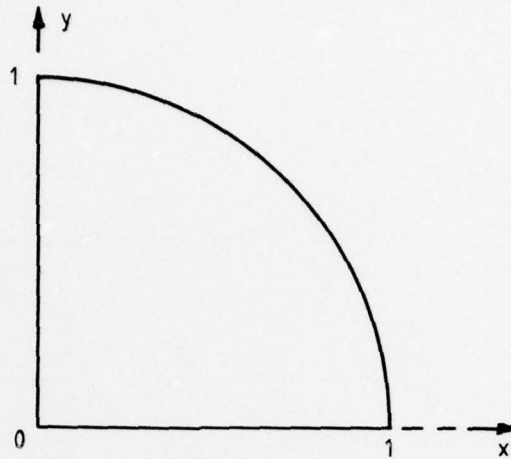
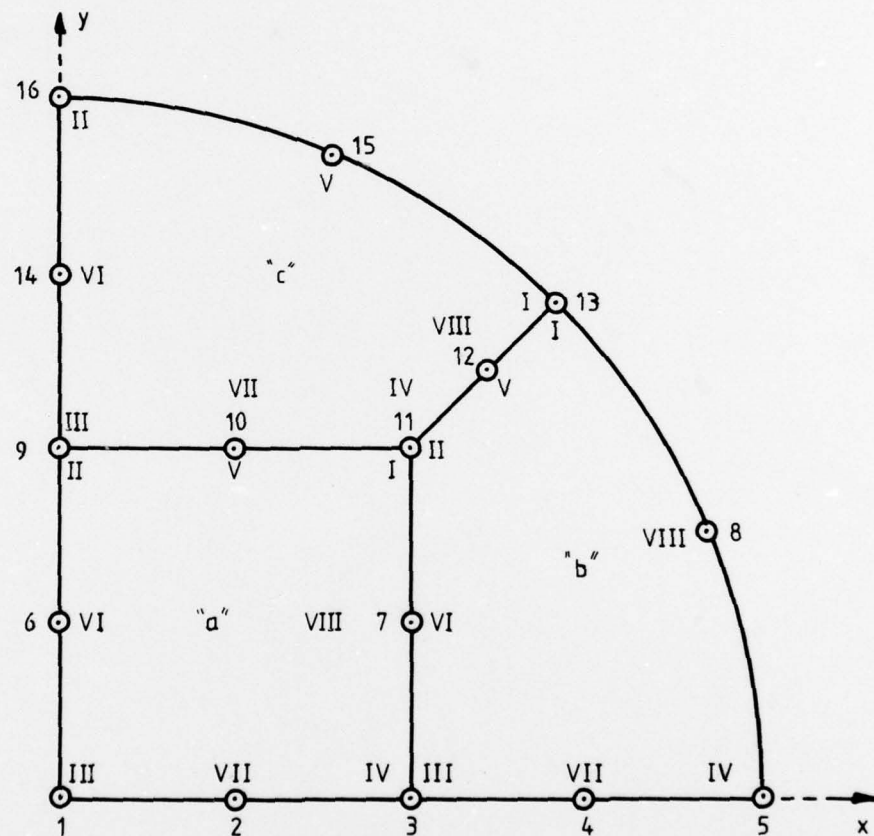


FIG. 10 CROSS SECTION OF BAR FOR ILLUSTRATIVE EXAMPLE OF SECTION 5



Global nodes numbered in ordinary numerals
Local (element) nodes numbered in Roman numerals

FIG. 11 FINITE ELEMENT SUBDIVISION, WITH NODAL NUMBERS, FOR ILLUSTRATIVE EXAMPLE OF SECTION 5

5.2 Mapping Functions

The mapping functions for the elements are obtained by substituting the values of x_i and y_i from Table 14 into Equations (2.3.12). However, since these are not required in the calculation, they will not be displayed here. (In any case, the accuracy of the mapping for the curved boundary has already been examined in Section (2.3.2). The derivatives of the mapping functions, which are required at the integration points ($\pm 1/\sqrt{3}$, $\pm 1/\sqrt{3}$) are shown below for each element; these are obtained by substituting from Table 14 into Equations (2.3.21). Also shown are the quantities J , A , B , and C for each element as calculated from Equations (2.3.3) and (3.4.3).

Element a

TABLE 15
Derivatives of Mapping Function for Element a

ξ, η	$-1/\sqrt{3}, -1/\sqrt{3}$	$1/\sqrt{3}, -1/\sqrt{3}$	$-1/\sqrt{3}, 1/\sqrt{3}$	$1/\sqrt{3}, 1/\sqrt{3}$
x_ξ	0.25	0.25	0.25	0.25
x_η	0	0	0	0
y_ξ	0	0	0	0
y_η	0.25	0.25	0.25	0.25

TABLE 16
Values of J , A , B , C for Element a

ξ, η	$-1/\sqrt{3}, -1/\sqrt{3}$	$1/\sqrt{3}, -1/\sqrt{3}$	$-1/\sqrt{3}, 1/\sqrt{3}$	$1/\sqrt{3}, 1/\sqrt{3}$
J	0.0625	0.0625	0.0625	0.0625
A	0.0625	0.0625	0.0625	0.0625
B	0	0	0	0
C	0.0625	0.0625	0.0625	0.0625

The simple form of these results is, of course, due to the fact that element a is a square so that here the mapping is simply of one square onto another.

Element b

TABLE 17
Derivatives of Mapping Function for Element b

ξ, η	$-1/\sqrt{3}, -1/\sqrt{3}$	$1/\sqrt{3}, -1/\sqrt{3}$	$-1/\sqrt{3}, 1/\sqrt{3}$	$1/\sqrt{3}, 1/\sqrt{3}$
x_ξ	0.2424	0.2424	0.1579	0.1579
x_η	-0.0137	-0.0514	-0.0480	-0.1795
y_ξ	0.0315	0.0315	0.0913	0.0913
y_η	0.2789	0.3581	0.2647	0.3051

TABLE 18
Values of J, A, B, C for Element b

ξ, η	$-1/\sqrt{3}, -1/\sqrt{3}$	$1/\sqrt{3}, -1/\sqrt{3}$	$-1/\sqrt{3}, 1/\sqrt{3}$	$1/\sqrt{3}, 1/\sqrt{3}$
J	0.0680	0.0884	0.0462	0.0646
A	0.0780	0.1309	0.0724	0.1253
B	0.0054	-0.0011	0.0166	-0.0004
C	0.0598	0.0598	0.0332	0.0332

Element c

There is no need to do any calculations for element c since it is symmetric with respect to element b.

5.3 Element Matrices

The values of the quantities u_i , v_i , and w_i at the integration points, as computed from Table 3, are shown in Tables 19, 20 and 21 below.

TABLE 19
Values of u_i at Integration Points

i ξ, η	$-1/\sqrt{3}, -1/\sqrt{3}$	$1/\sqrt{3}, -1/\sqrt{3}$	$-1/\sqrt{3}, 1/\sqrt{3}$	$1/\sqrt{3}, 1/\sqrt{3}$
I	-0.1830	0.0610	-0.2276	0.6830
II	-0.0610	0.1830	-0.6830	0.2276
III	-0.6830	0.2276	-0.0610	0.1830
IV	-0.2276	0.6830	-0.1830	0.0610
V	0.2440	-0.2440	0.9106	-0.9106
VI	-0.3333	-0.3333	-0.3333	-0.3333
VII	0.9106	-0.9106	0.2440	-0.2440
VIII	0.3333	0.3333	0.3333	0.3333

TABLE 20
Values of v_i at Integration Points

i ξ, η	$-1/\sqrt{3}, -1/\sqrt{3}$	$1/\sqrt{3}, -1/\sqrt{3}$	$-1/\sqrt{3}, 1/\sqrt{3}$	$1/\sqrt{3}, 1/\sqrt{3}$
I	-0.1830	-0.2276	0.0610	0.6830
II	-0.2276	-0.1830	0.6830	0.0610
III	-0.6830	-0.0610	0.2276	0.1830
IV	-0.0610	-0.6830	0.1830	0.2276
V	0.3333	0.3333	0.3333	0.3333
VI	0.9106	0.2440	-0.9106	-0.2440
VII	-0.3333	-0.3333	-0.3333	-0.3333
VIII	0.2440	0.9106	-0.2440	-0.9106

TABLE 21
Values of w_i at Integration Points

i	ξ, η	$-1/\sqrt{3}, -1/\sqrt{3}$	$1/\sqrt{3}, -1/\sqrt{3}$	$-1/\sqrt{3}, 1/\sqrt{3}$	$1/\sqrt{3}, 1/\sqrt{3}$
I		-0.0962	-0.1666	-0.1666	0.0962
II		-0.1666	-0.0962	0.0962	-0.1666
III		0.0962	-0.1666	-0.1666	-0.0962
IV		-0.1666	0.0962	-0.0962	-0.1666
V		0.1408	0.1408	0.5257	0.5257
VI		0.5257	0.1408	0.5257	0.1408
VII		0.5257	0.5257	0.1408	0.1408
VIII		0.1408	0.5257	0.1408	0.5257

The quantities a_{ij} and b_i can now be calculated for each element using Equations (3.4.7) and (3.4.8) in conjunction with the numerical values of Tables 16, 18, 19, 20 and 21. (The integration formula (4.1.2) is, of course, used.) Now the a_{ij} comprise the elements of a symmetric 8×8 matrix. The results for each element, after the conversion from element nodes to global nodes are shown in Equations (5.3.1), (5.3.2) and (5.3.3).

$$\begin{aligned} \text{Element } a \quad & \begin{bmatrix} \partial I_a / \partial \Psi_{11} \\ \partial I_a / \partial \Psi_9 \\ \partial I_a / \partial \Psi_1 \\ \partial I_a / \partial \Psi_3 \\ \partial I_a / \partial \Psi_{10} \\ \partial I_a / \partial \Psi_6 \\ \partial I_a / \partial \Psi_2 \\ \partial I_a / \partial \Psi_7 \end{bmatrix} = \begin{bmatrix} 1.111 & 0.500 & 0.555 & 0.500 & -0.777 & -0.555 & 0.500 & -0.777 & -0.555 & -0.777 \\ 0.500 & 1.111 & 0.500 & 0.555 & -0.777 & -0.777 & 0.555 & -0.777 & -0.555 & -0.555 \\ 0.555 & 0.500 & 1.111 & 0.500 & -0.555 & -0.777 & -0.777 & -0.777 & -0.555 & -0.555 \\ 0.500 & 0.555 & 0.500 & 1.111 & -0.555 & -0.555 & -0.777 & -0.777 & -0.555 & -0.777 \\ -0.777 & -0.777 & -0.555 & -0.555 & 2.222 & 0 & 0.444 & 0 & 0.444 & 0 \\ -0.555 & -0.777 & -0.777 & -0.555 & 0 & 2.222 & 0 & 0.444 & 0 & 0.444 \\ -0.555 & -0.555 & -0.777 & -0.777 & 0.444 & 0 & 2.222 & 0 & 2.222 & 0 \\ -0.777 & -0.555 & -0.555 & -0.777 & 0 & 0.444 & 0 & 2.222 & 0 & 2.222 \end{bmatrix} \begin{bmatrix} \Psi_{11} \\ \Psi_9 \\ \Psi_1 \\ \Psi_3 \\ \Psi_{10} \\ \Psi_6 \\ \Psi_2 \\ \Psi_7 \end{bmatrix} - \begin{bmatrix} -0.041 \\ -0.041 \\ -0.041 \\ -0.041 \\ 0.166 \\ 0.166 \\ 0.166 \\ 0.166 \end{bmatrix} \end{aligned} \quad (5.3.1)$$

$$\begin{aligned} \text{Element } b \quad & \begin{bmatrix} \partial I_b / \partial \Psi_{13} \\ \partial I_b / \partial \Psi_{11} \\ \partial I_b / \partial \Psi_3 \\ \partial I_b / \partial \Psi_5 \\ \partial I_b / \partial \Psi_{12} \\ \partial I_b / \partial \Psi_7 \\ \partial I_b / \partial \Psi_4 \\ \partial I_b / \partial \Psi_8 \end{bmatrix} = \begin{bmatrix} 1.348 & 0.758 & 0.622 & 0.472 & -1.563 & -0.653 & -0.735 & -0.249 \\ 0.758 & 1.623 & 0.572 & 0.700 & -1.527 & -0.667 & -0.871 & -0.586 \\ 0.622 & 0.572 & 1.084 & 0.564 & -0.846 & -0.627 & -0.998 & -0.371 \\ 0.472 & 0.700 & 0.564 & 1.188 & -0.794 & -0.522 & -1.203 & -0.405 \\ -1.563 & -1.527 & -0.846 & -0.794 & 3.137 & 0.528 & 1.113 & -0.047 \\ -0.653 & -0.667 & -0.627 & -0.522 & 0.528 & 1.908 & 0.034 & -0.000 \\ -0.735 & -0.871 & -0.998 & -1.203 & 1.113 & 0.034 & 2.812 & -0.152 \\ -0.249 & -0.586 & -0.371 & -0.405 & -0.047 & -0.000 & -0.152 & 1.813 \end{bmatrix} \begin{bmatrix} \Psi_{13} \\ \Psi_{11} \\ \Psi_3 \\ \Psi_5 \\ \Psi_{12} \\ \Psi_7 \\ \Psi_4 \\ \Psi_8 \end{bmatrix} - \begin{bmatrix} -0.045 \\ -0.052 \\ -0.044 \\ -0.036 \\ 0.160 \\ 0.163 \\ 0.195 \\ 0.193 \end{bmatrix} \end{aligned} \quad (5.3.2)$$

$$\begin{aligned} \text{Element } c \quad & \begin{bmatrix} \partial I_c / \partial \Psi_{13} \\ \partial I_c / \partial \Psi_{11} \\ \partial I_c / \partial \Psi_9 \\ \partial I_c / \partial \Psi_{16} \\ \partial I_c / \partial \Psi_{12} \\ \partial I_c / \partial \Psi_{10} \\ \partial I_c / \partial \Psi_{14} \\ \partial I_c / \partial \Psi_{15} \end{bmatrix} = \begin{bmatrix} 1.348 & 0.758 & 0.622 & 0.472 & -1.563 & -0.653 & -0.735 & -0.249 \\ 0.758 & 1.623 & 0.572 & 0.700 & -1.527 & -0.667 & -0.871 & -0.586 \\ 0.622 & 0.572 & 1.084 & 0.564 & -0.846 & -0.627 & -0.998 & -0.371 \\ 0.472 & 0.700 & 0.564 & 1.188 & -0.794 & -0.522 & -1.203 & -0.405 \\ -1.563 & -1.527 & -0.846 & -0.794 & 3.137 & 0.528 & 1.113 & -0.047 \\ -0.653 & -0.667 & -0.627 & -0.522 & 0.528 & 1.908 & 0.034 & -0.000 \\ -0.735 & -0.871 & -0.998 & -1.203 & 1.113 & 0.034 & 2.812 & -0.152 \\ -0.249 & -0.586 & -0.371 & -0.405 & -0.047 & -0.000 & -0.152 & 1.813 \end{bmatrix} \begin{bmatrix} \Psi_{13} \\ \Psi_{11} \\ \Psi_9 \\ \Psi_{16} \\ \Psi_{12} \\ \Psi_{10} \\ \Psi_{14} \\ \Psi_{15} \end{bmatrix} - \begin{bmatrix} -0.045 \\ -0.052 \\ -0.044 \\ -0.036 \\ 0.160 \\ 0.163 \\ 0.195 \\ 0.193 \end{bmatrix} \end{aligned} \quad (5.3.3)$$

5.4 Global Equations and Solution

The global equations as given by Equations (3.3.3) are obtained by the appropriate addition of Equations (5.3.1), (5.3.2) and (5.3.3). (For example, the equation $\partial I / \partial \Psi_{11} = 0$ is obtained by adding the first of (5.3.1), the second of (5.3.2), and the second of (5.3.3).) This leads to 16 equations in 16 unknowns. In the interests of brevity these will not be written down. After the application of the boundary conditions, which involves setting $\Psi_k = 0$ for all k save 7, 10, 11 and 12, and the discarding of the corresponding equations $\partial I / \partial \Psi_k = 0$, the reduced set of equations for solution becomes

$$\begin{bmatrix} 4.130 & 0 & -1.445 & 0.528 \\ 0 & 4.130 & -1.445 & 0.528 \\ -1.445 & -1.445 & 4.358 & -3.054 \\ 0.528 & 0.528 & -3.054 & 6.274 \end{bmatrix} \begin{bmatrix} \Psi_7 \\ \Psi_{10} \\ \Psi_{11} \\ \Psi_{12} \end{bmatrix} = \begin{bmatrix} 0.330 \\ 0.330 \\ -0.146 \\ 0.321 \end{bmatrix} \quad (5.4.1)$$

The solution of (5.4.1) is

$$\Psi_7 = 0.100, \Psi_{10} = 0.100, \Psi_{11} = 0.086, \Psi_{12} = 0.076 \quad (5.4.2)$$

Hence, on recalling the correspondence between global nodes and element nodes given in Table 14, it follows that, in element a,

$$\psi(\xi, \eta) = 0.086Q_I(\xi, \eta) + 0.100Q_V(\xi, \eta) + 0.100Q_{VIII}(\xi, \eta) \quad (5.4.3)$$

in element b,

$$\psi(\xi, \eta) = 0.086Q_{II}(\xi, \eta) + 0.076Q_V(\xi, \eta) + 0.100Q_{VI}(\xi, \eta) \quad (5.4.4)$$

and in element c,

$$\psi(\xi, \eta) = 0.086Q_{IV}(\xi, \eta) + 0.100Q_{VII}(\xi, \eta) + 0.076Q_{VIII}(\xi, \eta) \quad (5.4.5)$$

The torsion constant for each element is obtained using Equation (3.4.10). For example, for element a,

$$K_a = 0.086b_I + 0.100b_V + 0.100b_{VIII} \quad (5.4.6)$$

and, extracting the relevant values of b_i from Equation (5.3.1), gives

$$K_a = 0.0298$$

Analogous calculations for the other elements give

$$K_b = K_c = 0.0241$$

Summing the values for the elements gives the torsion constant for the complete section; the result is

$$K = 0.0781 \quad (5.4.7)$$

(The exact answer as given in Reference 8 is 0.0825.) The stresses τ_x and τ_y at node 13 will be calculated, treating this node as belonging to element b. Since global node 13 corresponds to local node I in element b, the following calculations are made with $\xi = \eta = 1$ in Equations (3.4.11). The derivatives of the mapping function, as obtained from Equations (2.3.21) take the values

$$\begin{aligned} x_\xi &= 0.1035 & x_\eta &= -0.2870 \\ y_\xi &= 0.1035 & y_\eta &= 0.2952 \end{aligned} \quad (5.4.8)$$

with the Jacobian $J = 0.0603$.

From Equation (3.4.4) and Table 3, it follows that

$$\psi_\xi = 0.086(1 + \eta)(2\xi - \eta)/4 + 0.076(-\xi)(1 + \eta) - 0.100(1 - \eta^2)/2$$

Hence,

$$\psi_\xi(1, 1) = -0.109 \quad (5.4.9)$$

An analogous calculation gives

$$\psi_y(1, 1) = 0 \quad (5.4.10)$$

Substituting from (5.4.8), (5.4.9) and (5.4.10) into Equations (3.4.11), with K having the value 0.0781 leads to the result

$$\tau_x/T = -6.67 \quad \tau_y/T = +6.86 \quad (5.4.11)$$

From considerations of symmetry it would be expected that the two stresses would be equal. Actually, if the calculation be repeated, now treating node 13 as belonging to element c, the results are reversed, i.e.

$$\tau_x/T = -6.86 \quad \tau_y/T = +6.67 \quad (5.4.12)$$

In general, there are discontinuities in the stresses at the boundaries of adjacent elements and, clearly, if mean values be taken here, the equality required by symmetry is restored.

6. OTHER APPLICATIONS OF ISOPARAMETRIC ELEMENTS

The two types of isoparametric elements described above can be used for a wide variety of two-dimensional problems in continuum mechanics. As well as problems in elasticity, problems in heat conduction, fluid mechanics, etc., can be solved. The discussion of Section 2 is applicable in all cases but, naturally, that of Section 3 must be replaced by the appropriate physical formulation.

It is possible to extend the concept to three-dimensional elements. One can develop an eight-node plane-sided cuboid which is the three-dimensional analogue of Figure 4 and a twenty-node curved-sided cuboid which is the analogue of Figure 5. However, particularly in the latter case, the analysis becomes formidable.

Reverting again to the two-dimensional situation, the application of the eight-node element has received considerable attention for the determination of the stress intensity factor at the tip of a crack in an elastic sheet.^{9,10} The procedures of References 9 and 10 differ somewhat and the following discussion is based on the latter reference. A wedge-shaped element (Fig. 12) is used and this is obtained by collapsing one side of an originally four-sided region into a single point, which is located at the crack tip. An important detail is that the intermediate nodes V and VII must be placed at one-quarter of the distance along each side from the crack tip. If the vertex angle be denoted by α , then the co-ordinates of the nodes are typically as shown in Table 22.

TABLE 22
Nodal Co-ordinates for Crack-Tip Element

Node	x_i	y_i
I	$\cos \alpha$	$\sin \alpha$
II	0	0
III	0	0
IV	1	0
V	$(\cos \alpha)/4$	$(\sin \alpha)/4$
VI	0	0
VII	1/4	0
VIII	$(1 + \cos \alpha)/2$	$(\sin \alpha)/2$

9. Henshell, R. D., and Shaw, K. G., Crack Tip Finite Elements are Unnecessary, *Inter. J. Numerical Methods in Engineering*, vol. 9, pp. 495-507, 1975.

10. Hussain, M. A., Lorensen, W. E., and Pflegl, G., The Quarter-Point Quadratic Element as a Singular Element for Crack Problems, *NASTRAN: Users' Experiences, Fifth Colloquium*, NASA TM X-3428, pp. 419-38, October 1976.

The region of Figure 12 is mapped on to that of Figure 3 using the standard transformation (2.3.12). On substituting the values of x_i and y_i from Table 22 into (2.3.12) it is found, after some trigonometric manipulations, that

$$x = (1 + \xi)^2 \{ \cos^2(\alpha/2) - \eta \sin^2(\alpha/2) \} / 4 \quad (6.1)$$

$$y = (1 + \xi)^2 (1 + \eta) \{ \sin(\alpha/2) \cos(\alpha/2) \} / 4$$

The Jacobian of this transformation is given by

$$J = (1 + \xi)^3 \sin \alpha / 16 \quad (6.2)$$

which, naturally, vanishes all along $\xi = -1$. Introducing polar co-ordinates r, θ given by

$$x = r \cos \theta, y = r \sin \theta \quad (6.3)$$

it is possible to invert Equations (6.1) to obtain

$$\xi = \{ 2r^{\frac{1}{2}} \cos^{\frac{1}{2}}(\theta - \alpha/2) \} / \{ \cos^{\frac{1}{2}}(\alpha/2) \} - 1 \quad (6.4)$$

$$\eta = \{ \tan(\theta - \alpha/2) \} / \tan \alpha/2$$

A displacement component, u , is taken to be given by the general formula analogous to Equation (2.2.5), i.e.

$$u = \sum_{i=1}^{VIII} Q_i(\xi, \eta) u_i \quad (6.5)$$

From this last, the formula for $u(\xi, \eta)$ can be obtained by setting $u_{II} = u_{III} = u_{VI} = 0$. If, in this formula—which will not be written down at length here—the substitutions (6.4) are made, it will be found that in the vicinity of the crack tip, where r is small, u is proportional to $r^{\frac{1}{2}}$. This is the characteristic behaviour required of a crack-tip element. For further details, reference should be made to the papers cited previously.

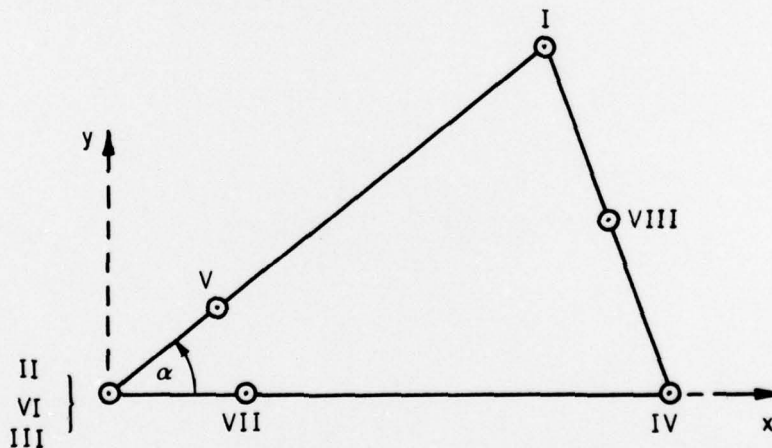


FIG. 12 ISOPARAMETRIC ELEMENT FOR DETERMINING STRESS INTENSITY FACTOR

7. CONCLUSIONS

The main point of the present work has been to exemplify, by means of particular problems treated in some detail, the use of isoparametric finite elements. Such elements can be gainfully employed in a wide variety of applications.

DOCUMENT CONTROL DATA SHEET

Security classification of this page: Unclassified

1. Document Numbers		2. Security Classification	
(a) AR Number: AR-001-292		(a) Complete document: Unclassified	
(b) Document Series and Number: Structures Report 372		(b) Title in isolation: Unclassified	
(c) Report Number ARL-Struc.-Report-372		(c) Summary in isolation: Unclassified	
3. Title: AN INTRODUCTION TO THE USE OF ISOPARAMETRIC ELEMENTS WITH EXAMPLES FROM THE TORSION PROBLEM			
4. Personal Author(s): Brian C. Hoskin Beryl I. Green		5. Document Date: August, 1978	
6. Type of Report and Period Covered:			
7. Corporate Author(s): Aeronautical Research Laboratories		8. Reference Numbers	
		(a) Task: DST 78/033 and AUS 63/01	
9. Cost Code: 21 6901 (75%) and 21 5020 (25%)		(b) Sponsoring Agency: Dept. of Defence (DSTO) and Dept. of Transport (ATG)	
10. Imprint: Aeronautical Research Laboratories, Melbourne		11. Computer Program(s) (Title(s) and language(s)):	
12. Release Limitations (of the document): Approved for public release			
12-0. Overseas:	No.	P.R.	1 A B C D E
13. Announcement Limitations (of the information on this page): No limitation			
14. Descriptors:		15. Cosati Codes: 1402	
Structural analysis	Bars	1313	
Torsion	Isoparametric elements		
	Finite element method		

16.

ABSTRACT

An introductory account is given of the use of isoparametric elements in finite element structural analysis. The basic theory is described and two simple examples are worked out in detail; these both relate to the torsion of bars. Brief mention is also made of other applications of isoparametric elements.

DISTRIBUTION

Copy No.

AUSTRALIA

DEPARTMENT OF DEFENCE

Central Office

Chief Defence Scientist	1
Executive Controller, ADSS	2
Superintendent, Defence Science Administration	3
Australian Defence Science and Technical Representative (UK)	4
Counsellor, Defence Science (USA)	5
Defence Library	6
Joint Intelligence Organization	7
Assistant Secretary, DISB	8-21

Aeronautical Research Laboratories

Chief Superintendent	24
Superintendent, Structures Division	25
Divisional File, Structures Division	26
Authors: B. C. Hoskin	27
B. I. Green	28
Library	29
D. G. Ford	30

Materials Research Laboratories

Library	31
---------	----

Defence Research Centre

Library	32
---------	----

Central Studies Establishment Information Centre

Library	33
---------	----

Engineering Development Establishment

Library	34
---------	----

RAN Research Laboratory

Library	35
---------	----

Navy Office

Naval Scientific Adviser	36
--------------------------	----

Army Office

Army Scientific Adviser	37
Royal Military College	38
US Army Standardisation Group	39

Air Office

Air Force Scientific Adviser	40
Aircraft Research and Development Unit	41
Engineering (CAFTS) Library	42
(D. Air Eng)	43
HQ Support Command (SENGSO)	44

DEPARTMENT OF PRODUCTIVITY

Government Aircraft Factories

Library 45

DEPARTMENT OF NATIONAL RESOURCES

Secretary, Canberra 46

DEPARTMENT OF TRANSPORT

Dep. Sec. (Air Operation)/Library 47

Airworthiness Group (Mr. R. Ferrari) 48

STATUTORY, STATE AUTHORITIES AND INDUSTRY

Australian Atomic Energy Commission (Director), NSW 49

CSIRO Central Office 50

CSIRO Mechanical Engineering Division (Chief) 51

CSIRO Tribophysics Division (Director) 52

Qantas, Library 53

Trans Australia Airlines, Library 54

SEC Herman Research Laboratory 55

SEC of Queensland 56

Ansett Airlines of Australia, Library 57

BHP Central Research Laboratories, NSW 58

BHP Melbourne Research Laboratories 59

Commonwealth Aircraft Corporation (Manager) 60

Commonwealth Aircraft Corporation (Manager of Engineering) 61

Hawker de Havilland Pty. Ltd. (Librarian) Bankstown 62

Hawker de Havilland Pty. Ltd. (Manager) Lidcombe 63

UNIVERSITIES AND COLLEGES

Adelaide Barr Smith Library 64

Professor of Mechanical Engineering 65

Australian National Library 66

Flinders Library 67

James Cook Library 68

La Trobe Library 69

Melbourne Engineering Library 70

Monash Library 71

Newcastle Library 72

New England Library 73

New South Wales Physical Sciences Library 74

Assoc. Prof. R. W. Traill-Nash, Struc. Eng. 75

Queensland Library 76

Sydney Professor G. A. Bird, Aero. Engineering 77

Professor R. Wilson, Applied Mathematics 78

Tasmania Engineering Library 79

Western Australia Library 80

RMIT Library 81

Mr. H. Millicer, Aeronautical Engineering 82

CANADA

CAARC Co-ordinator Structures 83

NRC, National Aeronautics Establishment, Library 84

NRC, Division of Mechanical Engineering (Dr. D. McPhail, Director) 85

UNIVERSITIES

McGill Library 86

Toronto Institute for Aerospace Studies 87

FRANCE		
AGARD, Library		88
ONERA, Library		89
Service de Documentation, Technique de l'Aeronautique		90
GERMANY		
ZLDI		91
INDIA		
CAARC Co-ordinator Structures		92
Civil Aviation Department (Director)		93
Defence Ministry, Aero. Development Establishment, Library		94
Hindustan Aeronautics Ltd., Library		95
Indian Institute of Science, Library		96
Indian Institute of Technology, Library		97
National Aeronautical Laboratory (Director)		98
INTERNATIONAL COMMITTEE ON AERONAUTICAL FATIGUE		
(Through Australian ICAF Representative)		99-121
ISRAEL		
Technion—Israel Institute of Technology (Professor J. Singer)		122
ITALY		
Associazione Italiana de Aeronautica and Astronautica (Professor A. Evla)		123
JAPAN		
National Aerospace Laboratory, Library		124
UNIVERSITIES		
Tohoku (Sendai) Library		125
Tokyo Institute of Space and Aerospace		126
NETHERLANDS		
Central Organization for Applied Science Research in the Netherlands TNO, Library		127
National Aerospace Laboratory (NLR) Library		128
NEW ZEALAND		
Air Department, RNZAF Aero Documents Section		129
Transport Ministry, Civil Aviation Division, Library		130
UNIVERSITIES		
Canterbury Library		131
SWEDEN		
Aeronautical Research Institute		132
Chalmers Institute of Technology, Library		133
Kungl. Tekniska Hogskolens		134
SAAB, Library		135
Research Institute of the Swedish National Defence		136
UNITED KINGDOM		
Mr. A. R. G. Brown, ADR/MAT (MAT)		137
Ministry of Power (Chief Scientist)		138
Aeronautical Research Council, NPL (Secretary)		139
CAARC NPL (Secretary)		140
Royal Aircraft Establishment Library, Farnborough		141
Royal Aircraft Establishment Library, Bedford		142

Royal Armament Research and Development Establ., Library	143
Aircraft and Armament Experimental Establishment	144
National Engineering Laboratories (Superintendent)	145
British Library, Science Reference Library	146
British Library, Lending Division	147
Naval Construction Research Establishment (Superintendent)	148
CAARC Co-ordinator, Structures	149
Aircraft Research Association, Library	150
British Ship Research Association	151
Central Electricity Generating Board	152
Rolls-Royce (1971) Ltd., Aeronautics Div. (Chief Librarian)	153
Hawker Siddeley Aviation Ltd., Brough	154
Hawker Siddeley Aviation Ltd., Greengate	155
Hawker Siddeley Aviation Ltd., Kingston-upon-Thames	156
Hawker Siddeley Dynamics Ltd., Hatfield	157
British Aircraft Corp. (Holdings) Ltd. Comm. A/craft Div.	158
British Aircraft Corp. (Holdings) Ltd. Military Aircraft	159
British Aircraft Corp. (Holdings) Ltd. Comm. Aviation Div.	160
British Hovercraft Corporation Ltd. (E. Cowes)	161
Fairey Engineering Ltd., Hydraulic Division	162
Short Brothers & Harland	163
Westland Helicopters Ltd.	164
UNIVERSITIES AND COLLEGES	
Bristol Library, Engineering Department	165
Cambridge Library, Engineering Department	166
Nottingham Library	167
Southampton Library	168
Strathclyde Library	169
Cranfield Institute of Technology Library	170
Imperial College The Head	171
UNITED STATES OF AMERICA	
NASA Scientific and Technical Information Facility	172
Sandia Group (Research Organisation)	173
American Institute of Aeronautics and Astronautics	174
Applied Mechanics Reviews	175
The John Crerar Library	176
Boeing Co., Head Office	177
Cessna Aircraft Co. (Mr. D. W. Mallonee, Exec. Engineer)	178
Lockheed Aircraft Co. (Director)	179
Metals Abstracts	180
McDonnell Douglas Corporation (Director)	181
United Technologies Corp., Pratt & Whitney Aircraft Group	182
Battelle Memorial Institute, Library	183
UNIVERSITIES AND COLLEGES	
Cornell (New York) Library, Aeronautical Laboratories	184
Florida Mark H. Clarkson, Dept. of Aero. Eng.	185
Illinois Professor N. M. Newmark, Talbot Labs.	186
Stanford Library, Dept. of Aeronautics	187
Wisconsin Memorial Library, Serials Dept.	188
Brooklyn Institute of Polytechnic Library, Polytech Aero. Labs.	189
California Institute of Technology Library, Guggenheim Aero. Labs.	190

79